Hindawi
Adsorption Science & Technology
Volume 2022, Article ID 9410266, 30 pages
https://doi.org/10.1155/2022/9410266

Review Article

A Comprehensive Insight on Adsorption of Polyaromatic Hydrocarbons, Chemical Oxygen Demand, Pharmaceuticals, and Chemical Dyes in Wastewaters Using Biowaste Carbonaceous Adsorbents

Hifsa Khurshid,[1] **Muhammad Raza Ul Mustafa**,[1,2] **and Mohamed Hasnain Isa**[3]

[1]*Department of Civil & Environmental Engineering, Universiti Teknologi PETRONAS, 32610 Seri Iskandar, Perak Darul Ridzuan, Malaysia*
[2]*Centre for Urban Resource Sustainability, Institute of Self-Sustainable Building, Universiti Teknologi PETRONAS, Seri Iskandar, 32610 Perak, Malaysia*
[3]*Civil Engineering Programme, Faculty of Engineering, Universiti Teknologi Brunei, Tungku Highway, Gadong, BE1410, Brunei Darussalam*

Correspondence should be addressed to Hifsa Khurshid; hifsa_18002187@utp.edu.my

Received 21 October 2021; Accepted 4 January 2022; Published 25 January 2022

Academic Editor: Silvano Mignardi

Recent trends in adsorption of hazardous organic pollutants including Polyaromatic Hydrocarbons (PAHs), Chemical Oxygen Demand (COD), Pharmaceuticals, and Chemical Dyes in wastewater using carbonaceous materials such as activated carbon (AC) and biochar (BC) have been discussed in this paper. Utilization of biomass waste in the preparation of AC and BC has gained a lot of attention recently. This review outlines the techniques used for preparation, modification, characterization, and application of the above-mentioned materials in batch studies. The approaches towards understanding the adsorption mechanisms have also been discussed. It is observed that in the majority of the studies, high removal efficiencies were reported using biowaste adsorbents. Regarding the full potential of adsorption, varying values were obtained that are strongly influenced by the adsorbent preparation technique and adsorption method. In addition, most of the studies were concentrated on the kinetic, isotherm equilibrium, and thermodynamic aspects of adsorption, suggesting the dominant isotherm and kinetic models as Langmuir or Freundlich and pseudo-second-order models. Due to development in biosorbents, adsorption has been found to be increasingly economical. However, application of these adsorbents at commercial scale has not been adequately investigated and needs to be studied. Most of the studies have been conducted on synthetic solutions that do not completely represent the discharged effluents. This also needs attention in future studies.

1. Introduction

Protection of the environment is of great concern and has gained a lot of attention over the years. In particular, it has been increasingly crucial to meet the demand of clean and safe water. Various types of contaminants are continuously being added into freshwater streams due to increased industrialization and urbanization. Sewage treatment plants, industrial discharges, agricultural discharges, and other anthropogenic activities are major causes of increasing water contamination. Water pollutants are broadly classified into organic and inorganic contaminants [1]. Organic contaminants include pesticides, plasticizers, fertilizers, hydrocarbons, biphenyls, phenols, detergents, oils, greases, pharmaceuticals, and plant and animal tissues [2, 3]. These contaminants are harmful even in small concentrations. Many treatment methods such as physical (i.e., filtration, electrodialysis, flotation, and adsorption), chemical (i.e., precipitation, chemical oxidation,

and electrochemical technologies), and biological (i.e., activated sludge, biological aerated filters, microbial capacitive desalination, and microalgae-based treatment) have shown the ability to remove hazardous substances from polluted water [4–7]. Adsorption is regarded as one of the most suitable techniques for wastewater treatment due to its low cost, high efficiency, less harmful secondary products, and ease of operation [8]. However, the efficiency of the method significantly depends on the adsorbent properties, i.e., surface area, pore size, pore diameter, and functional groups, etc. Traditionally, expensive activated carbons were used as adsorbents for removal of pollutants. Currently, the development of numerous novel adsorbents particularly from biomass waste has generated a lot of interest in researchers. Many studies have reported successful removal of water pollutants using economical biowaste adsorbents, e.g., tea waste [9, 10], palm tree leaves (Lee et al., [11]), corn silk [12], oil palm fruit [13], teff straw [14], rice husk [15], banana peels [16], rape straw [17], and mangosteen peels [18]. These adsorbents have gained attention recently because of the development in modification techniques, which enable the production of a large surface area and prominent physicochemical and biological properties ([19, 20]; L. Zhang et al., [21]). There is much interest among researchers to explore more materials and methods for the preparation of these economical biowaste adsorbents.

In this review, recent trends in the utilization of carbonaceous biowaste materials, viz., activated carbon (AC) and biochar (BC), their preparation and modification techniques, targeted pollutants, and their removal efficiencies in batch studies, have been discussed in detail for anthropogenic organic pollutant adsorption such as Polyaromatic Hydrocarbons (PAHs), Chemical Oxygen Demand (COD), Pharmaceuticals, and Chemical Dyes. The adsorption mechanism has also been discussed. Peer-reviewed articles published between 2010 and 2020 have been mainly considered. A few reviews have been published in this area concentrating on single pollutant or single adsorbent material. Even so, to date, few reviews outline the adsorption of a variety of pollutants, e.g., organic pollutants. This review will help researchers and planners in understanding the complete adsorption process including biowaste adsorbent preparation, application for various types of priority organic pollutant adsorption, and adsorption modelling.

2. Adsorbent Selection, Preparation, Modification, and Characterization

Adsorption is a well-known and effective technique for wastewater treatment. Choice of the starting material for adsorbent development is based on several factors. The material should be high in carbon and oxygen content; have strong abrasion tolerance, good thermal stability, small pore diameter, and high exposed surface area; and be easily accessible. Low-cost materials used as adsorbents have been derived from high carbon content plants, livestock, and other products, such as fruit wastes, rice husk, woods, seaweed, algae, peat moss, hair, and keratin [22]. Pollutants can be removed effectively by converting organic low-cost materials into carbonaceous adsorbents, e.g., AC and BC. Preparation, modification, and characterization techniques of these materials are discussed further in subsequent sections.

2.1. Preparation of Activated Carbon. Activated carbon (AC) is a widely utilized adsorbent for the treatment of wastewater and drinking water. It is prepared by chemical or steam activation of char that can be made of different materials such as fossils or biomass. Nowadays, due to the demand for affordable adsorbents, attempts are made to replace commercially available ACs by biomass waste-produced ACs, e.g., waste tea [23, 24], rice husk [25], and oak wood (Liu et al., [26]). These ACs are not only economical but also proven to be environmentally sustainable.

ACs are prepared by utilizing physical and chemical methods of activation followed by carbonization at high temperatures [23]. Common methods reported for preparation and activation of ACs have been presented in Table 1. Usual steps followed in the process are as follows: (i) pretreatment including washing, drying (air/oven), and cutting or grinding (powder/small particle size); (ii) carbonization (in furnace/reactor with or without N_2 gas); (iii) activation/modification before or after carbonization (steam/acid/oxidizing agent/CO_2 gas); and (iv) posttreatment, e.g., washing (until pH is neutral) and drying (air/oven). Various acidic, basic, and oxidizing modification techniques have been reported in the literature for AC preparation. Activating agents produce ACs with improved properties including large porosity, high surface area, variety of functional groups, increased adsorption potential, and regeneration capability. Table 1 shows that surface area of AC may increase or decrease after modification depending on the feedstock properties and activating agent as well. Baghdadi et al. [27] stated that treatment of AC with nitric acid resulted in degradation of porous framework and modification of the AC exterior framework. On the other hand, carboxylic functional groups were introduced because of the treatment by nitric acid in the AC system. It enhanced the hydrophilicity of AC and consequently reduced the attraction for hydrophobic pollutants towards the adsorbent. Phosphoric acid and steam modifications have shown larger impact on surface area and pore size enhancement of ACs in most of the studies. Furthermore, ACs have also been reported to be modified by metal impregnation, e.g., silver, chromium, or copper [28], and thermal tension treatment to increase the porosity/surface area [29].

2.2. Preparation of Biochar. Biochar (BC) is a rich carbon compound developed through combustion at mild temperatures (300–700°C) under minimal to no oxygen condition [30] or as a byproduct of biocrude oil production [31]. Land wastes, crop residues, and the renewable components of industrial solid wastes have become major source materials for BC preparation. BC has been used to increase soil consistency, promote carbon sequestration, and immobilize pollutants [32]. Its properties rely on the type of raw material, combustion temperature, and residence time. Usually, BCs formed at high temperatures have a higher surface area and carbon content, primarily due to the rise in the number of micropores induced by the removal of volatile organic

Table 1: Preparation techniques for AC and BC utilizing various materials.

	Pretreatment	Activation method	Pyrolysis method	Posttreatment	Physical properties				Ref.
					Surface area (m^2/g)	Pore vol. (cm^3/g)	Ash content	FTIR functional groups	
Activated carbon (AC)									
Oil palm shell	Washed, dried overnight at 105°C, cut into mesh size of 1–2 mm	Char soaked in KOH solution (1 : 1) Activated at 700°C (10°C/min) to a final temperature of 850°C CO_2 switched and activation held for 2 hr	Carbonized at 700°C for 2 hr at heating rate of 10°C/min under purified nitrogen flow of 150 cm^3/min	Cooled to room temperature under nitrogen flow Washed with hot deionized water and 0.1 molar HCl until the pH of the washing solution reached 6–7	596.2	0.34		O–H stretching vibrations C ≡ C stretching vibrations C=C stretching vibration in aroma: C–OH stretching vibrations	[8]
Oil palm frond	Cut into small pieces (2 cm ×2 cm) Washed with water Dried at 105°C Crushed and sieved to mesh size of 1–4 mm	Char soaked in KOH solution (1 : 1, *w*/*w*%) for 24 hr Dehydrated in an oven overnight at 105°C	Carbonized at 700°C for 2 hr at heating rate of 10°C/min under purified nitrogen flow of 150 cm^3/min	Cooled to room temperature under nitrogen flow Washed with hot DI water and 0.1 molar HCl until the pH was neutral					[42]
Palm tree leaves	Washed with deionized water, air-dried, and cut into small pieces	Soaking dried small pieces in 25% (*w*/*w*) H_2SO_4 at room temperature for 24 hr	Carbonization in oven at different temperatures for 24 hr	Cooled the AC to room temperature Washed with deionized water Dried at 105 ±1°C for 12 hr Ground and sieved to particles between 300 μm and 425μm in size	64.12	0.0835		Hydroxyl (–OH) Bands of aliphatic C–H Band of carboxyl group (C=O) in carboxylic acid Bands of C=O (in -COO^-) or C=C centering ν(O–H), ν(C–H), and ν(C=O) vibrations	[43]
Waste rice straw	Washed, air-dried, and cut into small pieces	Steam penetrated the reactor at a pace of 5 mL/min as the furnace hit 350°C and the heating proceeded for 1 hr until the final temperature was 550, 650, & 750°C	0.5 kg dried rice straw fed into fluidized bed reactor, at heating rate 50°C/10 min in the presence of N_2 flow (300 mL/min)	Cooled down and washed with distilled water Dried at 120°C and stored					[44]

Table 1: Continued.

	Pretreatment	Activation method	Pyrolysis method	Posttreatment	Physical properties				Ref.
					Surface area (m^2/g)	Pore vol. (cm^3/g)	Ash content	FTIR functional groups	
Pecan shell	Washed, air-dried, and cut into small pieces	Steam activated at 900°C for 6 hr CO_2 activated at 900°C for 6 hr H_3PO_4 activation at 170°C for 6 hr	Carbonized at 700°C	Cooled down and washed	917 ± 5 435 ± 39 902 ± 4		5.53 ± 0.16 6 ± 0.08 1.42 ± 0.01		[45]
Tea industry waste	Dried and ground to less than 150 μm size	20 g of tea wastes and 20 g of $ZnCl_2$ mixed (1 : 1) A portion of 150 mL of distilled water added to the mixture and allowed to stand for 1 day Solution was filtered	Carbonized in furnace starting at room temperature and increased to 700°C in 80 min under nitrogen at flow rate of 100 mL/min and maintained for 4 hr	Cooled to room temperature under nitrogen atmosphere 2 times boiled in 2 M HCl and filtered Dried at 105°C for 4 hr and kept in desiccator	1066	0.58	1.04		[46]
Rice husk	Washed, air-dried, and cut into small pieces	Impregnated 40g of rice husk with 100 mL of 40% (*v*/*v*) H_3PO_4	Heated up to 673 K in 2 hr and then held at this temperature for 3 hr	Cooled by washing until the pH became 6.5 The mass dried at 110°C	446				[47]
Tea waste	Washed with distilled water Dried in oven at 60°C Ground and sieved by mesh size of 60 μm	Carbon precursor was impregnated with 85% H_3PO_4 by varying the chemical ratio from 1 : 1 (*w*/*v*) to 1 : 3 and kept in oven at 60°C for 3 hr with occasional stirring	Carbonized at 400°C heating rate fixed on 5°C/min	Cooled down and washed initially with 0.1 M HCl and then with distilled water Dried at 110°C for 24 hr and stored in desiccator	2054.4 (1 : 3)	1.747 (1 : 3)			[48]
Date stones	Washed with distilled water. Dried in oven at 120°C. Crushed and ground to particle size of 0.5-1 mm	The precursor was impregnated with KOH in a solid form (9 mmol : 1 g date stones) was activated at 800°C The precursor was impregnated	The impregnated precursor was carbonized in a horizontal tubular furnace under nitrogen flow with a heating rate of 5°C/min for 1 h	The AC was immersed in HCl solution (0.1 M/L) for 3 hr Filtered and washed with hot distilled water Dried at 120°C and kept in	1209 1235	0.550 0.630		Hydroxyl groups with hydrogen bending of adsorbed water Aliphatic bond –CH, $-CH_2$, and $-CH_3$, aromatic C-C ring	[49]

Table 1: Continued.

	Pretreatment	Activation method	Pyrolysis method	Posttreatment	Physical properties				Ref.
					Surface area (m^2/g)	Pore vol. (cm^3/g)	Ash content	FTIR functional groups	
		with $ZnCl_2$ in a solid form (1 : 1) and activated at 600°C.		tightly closed bottles				–COO–, $–CH_3$ group, C–O	
Tea waste	Boiled multiple times with distilled water Washed and oven-dried at 103°C for 24 hr	Dried tea waste was modified by $ZnCl_2$, K_2CO_3, KOH, and H_2SO_4 in 1 : 1 (*w*/*w*) overnight at room temperature Filtered and dried in an oven at 103°C for 24 hr	Carbonized the activated material at 600°C for 2 hr	Washed and dried in an oven	865.4 483.9 416.4 116.2	0.5032 0.2222 0.2155 0.044		O-H & N-H stretching C-H stretching of alkanes and alkenes, carbonyl group (C=O) C=C vibrations in aromatic rings C-O stretching of alcohols	[50]
Wood sawdust	Ground and sieved to obtain a particle size of 0.5-1 mm	*Before carbonization*: chemically activated by KOH, and thermally activated under CO_2 gas flow for 2 hr *After carbonization*: impregnated the calcium solution of eggshell and AC (1 mL : 0.02 g) at required temperature	Carbonized in a horizontal furnace at 750°C under N_2 atmosphere (150 mL/min)	Cooled and washed with boiled deionized water until neutral pH Dried at 110°C for 24 hr *After impregnation*: cleaned with hot distilled water and dried at 110°C for 24 hr	*Before impreg.*: 678.641 *After impreg.*: 433.486				[51]
Waste tires	Cleaning, washing, and drying	Treatment using 4.0 M/L HNO_3 (1 : 20 g/mL) at 90°C for 3 h in a reflux condenser	7g AC-COCl was mixed with 100 mL of PEI solution. For 24 hr, the mixture was stirred at 150 rpm in a shaker at about 90°C.	Filtered, washed with distilled water, and dried at 110°C	363				[52]

Table 1: Continued.

	Pretreatment	Activation method	Pyrolysis method	Posttreatment	Physical properties				Ref.
					Surface area (m^2/g)	Pore vol. (cm^3/g)	Ash content	FTIR functional groups	
Biochar (BC)									
	Washed and air dried Crushed and ground to <1.0 mm size		Pyrolyzed at 300 and 700°C (7°C/min), with and without N_2 purging (5 mL/min)	Washed and dried Obtained: BC-300 BC-700 BC-300N BC-700N	2.28 342.22 0.90 421.31	0.0059 0.0219 0.0074 0.0576	5.69 10.87 5.87 11.60		
Tea waste		Steam activation: Samples were processed for an extra 45 min at maximum temperature with 5 mL/min of steam after the 2 hr pyrolysis cycle had passed.		Washed and dried. Obtained: BC-300S BC-700S	1.46 576.09	0.0042 0.1091	6.42 16.73	O-H stretching band, aliphatic CAH stretching band, PO_4^{3-}, and CO_3^{2-}	[10]
Tea waste	Washed and dried in oven at 60°C for 48 h Ground to <1 mm particle size		Pyrolyzed gradually at 700°C for 3 h with minimal oxygen at 7°C/min	Cooled down overnight in furnace	342.22	0.02	12.84		[15]
Rice husk	Washed and air-dried Ground to <1 mm particle size				377	0.05	39.24		
Banana peels	Washed and ground into 0.05 cm size	Soaked 4 g of raw material in 50 mL H_3PO_4 solutions for 2 hr at 0, 10, 20, 30, 40, & 50% concentration	The mixture was transferred to an autoclave and heated for 2 hr at 230°C	Dried overnight in oven at 80°C	45.27 36.85 31.65 31.54 30.91 28.80			H-bonding hydroxyl groups, -CH_2 or CH_3 groups in carboxylic acid, C=O (C-O) stretching vibration of carboxyl groups	[16]
Rape straw	Cleaned and dried	10 g biochars mixed separately with 1 L solution of 25% HNO_3 (v/v), 25% H_2O_2 (m/m), and 5%	Pyrolysis at 500°C in a high temperature furnace	Cleaned with water Dried at 80°C for 24 hr in an oven	2.44 2.39 2.62 90.2		5.15 1.68 3.52 44.5	Vibration of free hydroxyl group, associative hydroxyl group, C=O of carboxylic acid, and C=C of aromatic ring	[17]

Table 1: Continued.

	Pretreatment	Activation method	Pyrolysis method	Posttreatment	Physical properties				Ref.
					Surface area (m^2/g)	Pore vol. (cm^3/g)	Ash content	FTIR functional groups	
		$KMnO_4$ (m/m) Then stirred for 4 hr at 40°C in a magnetic stirrer							
Miscanthus × giganteus	Washed and dried	H_2O_2 10% w/v	Carbonized at 350 and 600°C.	Washed and dried	6.50 at 600°C	0.95			[35]
Dewatered sewage sludge	Dried at 105°C for 24 h and sieved into powder of 0.15-0.18 mm size	Using a magnetic stirrer at 12 0 rpm at RT for 12 h, 12 g material powder and 12 g ultrafine dolomite powder were combined with 75 mL DI water Put in a thermostat water-bath at 80°C and mixed for 2.5 h Dried overnight in the oven at 105°C	Pyrolyzed at 5°C/min till temp. reached 800°C and held for 2 h under N_2 purging	Washed and dried in oven	49.45	0.07		Vibrations of the hydroxyl groups (-OH)	[39]
					11.31	0.03		Vibrations of the hydroxyl groups (-OH) Mg-O and O-Mg-O vibration bands	
Peanut hull	Naturally dried Peanut hull mixed with DI water (3 : 20, w/v)	3 g of the carbonized sample placed into 20 mL 10% H_2O_2 solution for 2 hr at room temperature	Carbonize the mixture in autoclave held at 300°C for 5 hr at a pressure of about 1000 psi	Washed with DI water and dried at 80°C in an oven Ground and sieved to a uniform size fraction of 0.5–1.0 mm	1.3	0.24 0.25		Carbonyl groups	[53]
Colocasia esculenta	Cut into homogenous size, washed and dried for 2 days under sunlight Later dried in hot air oven over night at 100°C	Passed superheated steam at rate of 1.5 kg/cm^2 at 700°C for 45 min After 45 min of steam flow, the lag phase was sustained for 20 min at 700°C	Carbonized in a spherical shelled muffle furnace at 350-600°C for 45 min and maintained the temperature for 40 min	After carbonization, the temperature increased up to 700°C at 10°C/min. for activation Activated sample was ground into particle size of 450 μm			3.67	Carboxylic acids, aldehydes and aromatic groups, terminal alkynes, alcohols and phenols	[54]

Table 1: Continued.

	Pretreatment	Activation method	Pyrolysis method	Posttreatment	Physical properties				Ref.
					Surface area (m^2/g)	Pore vol. (cm^3/g)	Ash content	FTIR functional groups	
Lemon grass	Washed and dried	After carbonization sieved to 2 mm size The final biochar added into 50 mL H_2O_2 solutions with different concentrations (v/v—10%, 20%, 30%) for 3 hr at room temperature	Hydrothermal carbonization (10 g) was done with DI-water (w/w 1 : 1) at heating rate of 10°C/min. up to 200°C	Washed repeatedly Oven dried at 60°C overnight Ground into small sizes	27.2 26.9 27.3 27.1	0.533 0.537 0.541 0.548			[55]
Corn straws	Washed and dried	Dry corn straw (20 g) was impregnated with 35.6 mL 85% H_3PO_4 for 24 hr Dried in the oven at 105°C for 7 hr	Oven dried material was pyrolyzed in a furnace to heat at 10°C/min to 300°C and held for 2 hr	Washed Ground to 0.21 mm	1028.88	0.5378	4.01	OH groups, alkyl CH_2 stretching, aromatic carboxyl groups, aromatic C=C and C=O, C=C in guaiacyl lignin, C=O of carboxylate ions, hydroxyl bending vibration, OH in phenolic	[56]
Tea waste	Washed and dried in oven at 105°C Crushed to powder		Heated at 673 K for 1/2 h	Cooled down to room temperature Grounded to a powder of 0.2 mm size	5.07	0.0079			[57]
		H_2SO_4 followed by $NaNO_3$ were added to the dried biochar $KMnO_4$ was then added to the mixture with continuous stirring	Gradually heated from 323 K to 373 K and later 30% H_2O_2 added to the heated mixture and ultrasonicated for 15 min and filtered	Washed with distilled water for removal of excess acid; the resulting powder was dried in oven, grounded, sieved, and stored	11.833	0.0158		O-H bond stretching, C=C and C=O bonds stretching, C-O-C symmetric stretching	
Spent P. ostreatus substrate Spent shiitake substrate	Air dried and screened (40-mesh sieve)		Carbonized in furnace for 2 hr at temp. 300°C, 500°C, and 700°C in	Washed and dried	3.79 18.05 188.57 12.97 47.07 218.70	0.014 0.061 0.134 0.028 0.070 0.138	33.27 52.35 55.71 28.02 35.67 42.28	Aromatic C-H groups C-O/C-O-C stretching vibrations of alcohols,	[58]

Table 1: Continued.

	Pretreatment	Activation method	Pyrolysis method	Posttreatment	Physical properties				Ref.
					Surface area (m^2/g)	Pore vol. (cm^3/g)	Ash content	FTIR functional groups	
			oxygen-limited atm					phenols, and ether or ester groups, C=C ring stretching vibration	
Corn stalks	Dried in oven at 80°C (24 h) Crushed into powder	Crushed straw impregnated with 1.2 M K_2CO_3 solution (1 : 3, *w*/*v*) Dried at 80°C for 24 hr	Pyrolyzed in the furnace for 2 hr at 600°C	Ground and screened to <0.25mm size	680.36				[59]
Municipal sewage sludge and tea waste	Air-dried the sludge and tea waste, sieved, and meshed (100 size) Mixed both waste (1 : 1)		Pyrolyzed in muffle furnace at 300°C for 2 h	Cooled the biochar and sieved (100-mesh size)				OH groups Aliphatic C-H group C=O and C=C aromatic vibrations C=O and C=H stretching vibrations	[60]
Pinewood biomass	Cut into small pieces and dried at 105°C in oven	Biochar soaked in H_2O_2 solution (1, 3, 10, 20, 30%, *w*/*w*, 1 g : 20 mL).	Pyrolyzed at 400°C and held for 30min Cooled down with N_2 purging	Washed and dried at 105°C overnight				(C=C), carboxylic acid functionality, C-H stretching	[61]
Enteromorpha prolifera	Washed, air-dried, ground, and sieved (2 mm mesh)	Biochar soaked in HCl (1 M/L) and HF (40% w) mixture (180 : 20 mL) for 24 h	Pyrolyzed at 200–600°C with rate 10°C/min for 2 h under N2 purging (25mL/min)		205.32			Stretching of O–H in carboxyl and phenol functional groups, N–H symmetric stretching vibration, stretching of C=C and C=O	[62]
Miscanthus floridulus	Washed and dried in oven at 60°C Crushed and sieved (0.15–0.25 mm)		Pyrolyzed for 6 h (5°C/min) at 450°C and kept for 1 h under N_2 purging	Cooled and soaked in 1 M HCl for 12 h and washed				–OH groups, carbonyl/carboxyl (C=O), ether bond (C-O-C), C–O of phenolic group	[63]

compounds at high temperatures. However, as the temperature increases, the biochar yield decreases. Thus, in terms of biochar yield and adsorption capacity, an optimal strategy is needed. High temperature BCs are stable in both abiotic and biotic incubations, whereas BC from woody materials have more stable carbons than those generated from rice residues [33]. Amarasinghe et al. [34] stated that temperature range of 450°C to 500°C and residence time between 45 and 60 minutes had the fastest recovery in BC mass of tea waste. Increased pyrolysis temperature causes reduction in

hydrogen and oxygen content while carbon content increases resulting in reduced H/C and O/C ratios at higher temperatures [35]. Yin et al. [36] observed that when the temperature of pyrolysis rose from 300 to 700°C, BC yield decreased, while pH value, surface area, total pore volume, and ash amount increased. The drop in yield at high pyrolysis temperatures can be attributed to the decrease of volatile components, and the BC's high ash content suggested the aggregation of inorganic minerals that could elevate the pH and cation exchange capacity (CEC).

BC has a large percentage of organic carbon composition with rich oxygen-containing groups and can provide different sites of adsorption for heavy metal ions and aromatic pollutants. However, BC typically have smaller surface area compared to AC. Through utilizing chemical agents such as acids, bases and oxidizing agents and physical activation methods, the surface area and adsorptivity of the BCs can significantly improve. The modification methods enhance the porosity and add various functional groups at the surface of BC. Table 1 shows that usually acidic modification, e.g., HCl, K_2CO_3, and H_2SO_4, introduces O-H or carbon-based functional groups at the surface of the BC which may increase or decrease the surface area, whereas oxidizing agents such as H_2O_2, H_3PO_4, and HNO_3 introduce hydroxyl and carboxyl groups at the surface of BC increasing the negative charge at the surface. Wang and Liu [37] reported 63.4% and 101% rise in oxygen and carboxyl group content, respectively, in manure BC after modification by H_2O_2. Jin et al. [38] used HNO_3 to modify BC and found a very high adsorption of uranium due to increased content of carboxyl groups at the surface after modification. Many lamellar structures appeared on the surface of the dolomite-modified BC as compared with the raw BC, which provided binding sites for phosphate ions in solution [39]. Dolomite was decomposed into calcium and magnesium oxides probably due to the creation of the lamellar system. Luo et al. [40] used a unique method of BC modification through lignin modification by introducing acrylonitrile into the biochar prepared at various temperatures. It was observed that the BC prepared at 350°C was successfully modified and further utilized for metal adsorption in wastewater. However, at higher temperatures, lignin was not able to be modified. Common methods for preparation and activation of BC have been stated in Table 1. Usual steps involved in preparation include the following: (i) pretreatment, e.g., washing (repeatedly), drying (air/oven), and cutting or grinding (powder/small particle size); (ii) pyrolysis (in furnace/reactor with or without N_2) at various temperatures; (iii) modification before or after pyrolysis (steam/acid/bases/oxidizing agent); and (iv) posttreatment, e.g., washing (until pH is neutral) and drying (air/oven). Innovative methods such as ammoniation hydrothermal method have also been introduced recently for BC preparation [41]. Table 1 shows that generally, ACs have much higher surface areas as compared to BCs, but the preparation method of BC is simpler and more economical compared to AC.

2.3. Characterization Techniques. Characterization methods help in identifying the surface properties of the materials and impact of modification on material properties. Figure 1 presents commonly used methods for characterization of adsorbents. Scanning electron microscopy (SEM), scanning electron microscopy coupled with energy-dispersive spectroscopy (SEM–EDS), transmission electron microscopy (TEM), X-ray photoelectron spectroscopy (XPS), Brunauer–Emmett–Teller (BET) analysis, field-emission scanning electron microscopy (FESEM), Fourier transform infrared spectroscopy (FTIR), surface area analyzer and porosimetry system (SAAPS), gas chromatography mass spectrometry (GCMS), and X-ray diffraction (XRD) are widely used characterization methods for adsorbents. 129Xe NMR has been used as a modern technique for analysis of adsorption mechanism using a porous structure and channel measurement in adsorbent materials [64]. Based on Soxhlet extraction, sodium hydroxide (NaOH) procedure, and two-step acid hydrolysis cycle, respectively, the extractives, hemicellulose, and lignin content of the raw biomass can be evaluated (Lee et al., [11]).

3. Application of AC and BC for Adsorption of Organic Pollutants

Application of adsorbents is studied under various controlling parameters such as pH, contact time, initial concentration of adsorbate, temperature, and dosage of adsorbent. The effect of these parameters is commonly studied in batch experiments. The pH at which the charge on the adsorbent surface is zero is called the pH at zero-point charge (pH_{ZPC}). It is determined by plotting $pH_{initial}$ against pH_{final}, and the point where $pH_{initial} = pH_{final}$ is called pH_{ZPC} [65]. Below this pH, the material is supposed to be positively charged and favorable for anion adsorption, while above this pH, cations can be removed favorably. The pH and pH_{ZPC} of AC or BC can change with change in pyrolysis temperature [66]. Other parameters are highly adsorbent and pollutant dependent and change accordingly. Table 2 shows the summary of various input and optimized parameters studied in batch experiments and resulting maximum removal efficiencies for organic materials using AC and BC. The uptake capacity or removal efficiency of pollutants can be calculated by the following equations [67]:

$$q_e = \left(C_i - C_f\right) \times \frac{V}{M}, \tag{1}$$

$$\%\text{age removal} = \frac{C_i - C_f}{C_i} \times 100, \tag{2}$$

where q_e is the potential for adsorption at equilibrium in mg/g, C_i represents the initial concentration of pollutants in mg/L, C_f represents the final amount of adsorbate at equilibrium in mg/L, V is the volume of solution in L, and M represents the mass of adsorbent in g.

3.1. Activated Carbon. Organic pollutants, e.g., pharmaceuticals, dyes, and hydrocarbons, have been widely removed using biomass waste-produced ACs. Increased adsorption of organic compounds on AC is due to its large specific

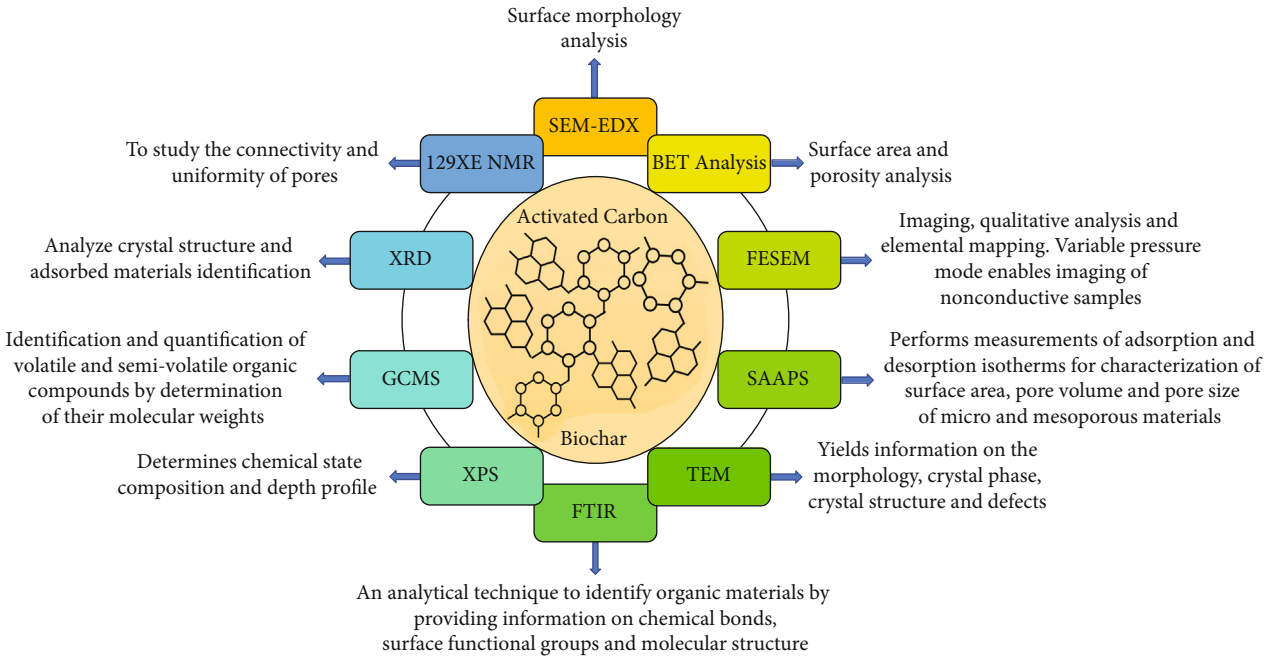

Figure 1: Characterization methods used for analysis of AC and BC.

surface area and attractive physicochemical properties such as high mechanical strength, chemical stability in different media, and large pore size [42]. Different organic pollutant adsorption by AC and its composites are discussed here. Organic pollutants such as pharmaceuticals, dyes, and hydrocarbons have been effectively removed from aqueous solutions using biomass waste-produced ACs. Amstaetter et al. [68] found that biomass-based AC showed stronger adsorption of organic compounds, e.g., PAHs and polychlorinated biphenyls (PCBs) as compared to anthracite-based AC. Increased adsorption of organic compounds on AC is attributed to its large specific surface area and attractive physicochemical properties such as high mechanical strength, chemical stability in different media, and large pore size [42].

3.1.1. Chemical Dyes. Organic chemical dyes such as methylene blue (MB), crystal violet, reactive blue 19, and thionine are used in various industrial processes. Textile, paper, plastics, leather, and printing industries release a large amount of the dyes in wastewater. These dyes are toxic, cause water pollution, and need to be treated on a priority basis. In excess amounts, they may block the necessary oxygen and sunlight penetration into water bodies causing death of aquatic life. The dyes usually have a complicated aromatic structure and are resistant to degradation by chemical, physical, and biological treatments. Being economical and efficient, adsorption is a potential treatment strategy for the removal of dyes from waste effluents [69].

Methylene blue is a commonly used cationic colouring dye. If swallowed or inhaled, it can cause gastrointestinal irritation, nausea, vomiting, diarrhea, cyanosis, and dyspnea. It also causes eye irritation and burning [8]. Borah et al. [48] studied adsorption of methylene blue (MB) and eosine yellow (EY) on tea waste-produced porous carbon. The tea waste was activated by phosphoric acid and adsorption of up to 99% was achieved for both dyes. The maximum monolayer adsorption was 402.25 mg/g and 400 mg/g for MB and EY, respectively, which is much higher than many adsorbents reported in literature, e.g., coconut shell (277.90 mg/g), Rattan-AC (294.12 mg/g), walnut shell-AC (3.53 mg/g), groundnut shell (164.90 mg/g), and granular AC (101.626 mg/g). It was found that AC loaded with nickel sulfide nanoparticles showed 99.9% removal of MB and safranin-O (SO), i.e., 46 and 52 mg/g at optimum condition of pH (8.1), adsorbent dosage (0.022 g), initial concentration of dyes (17.8 mg/L and 5 mg/L), and contact time (5.46 min) [69]. Another study reported development of a high surface area (854.30 m^2/g) waste tea AC by chemical activation with potassium acetate for adsorption of MB and Acid Blue 29 (AB29) dyes [70]. The AC was developed at optimized values of impregnation ratio, activation temperature, and activation time that were 1 : 4, 800°C, and 120 min, respectively. The adsorption capacities for MB and AB29 were 554.30 mg/g and 453.12 mg/g, respectively, which were higher than KOH-modified oil palm shell AC, i.e., 243.90 mg/g, and raw fruit AC, i.e., 146 mg/g, for MB [71]. Another study reported the optimized conditions for the synthesis of $ZnCl_2$-activated AC as follows: 1 : 4 impregnation ratio, calcination temperature of 600°C, and calcination time of 30 min [72]. The precursor material of AC synthesis was mangosteen peels, and a very high surface area of 1621.8 m^2/g was reported. For methylene blue, the adsorption potential of AC prepared under controlled conditions was 1193 mg/g. Nasrullah et al. [73] reported the synthesis of a high surface area (890 m^2/g) AC-alginate by inserting AC powder extracted from mangosteen fruit peel into calcium-alginate beads. The AC-alginate was used for the removal of MB from aqueous solution. The findings showed

Table 2: Application of AC and BC for adsorption of organic pollutants in batch studies.

Material	Sample	Pollutant	Adsorption batch study	pH	Initial conc. Of adsorbate (mg/L)	Contact time	Adsorbent dosage	Temp.	Adsorption mechanism	Max removal efficiency	Ref.
Oil palm frond (AC)	Aqueous solution	2,4-Dichlorophenoxyacetic acid	200 mL 2,4-D solutions (30°C) shaken in water-bath at 120 rpm for 24 hr	2-12	50–300	5 min-30 hr	50-300 mg/L	30, 40, and 50°C	Adsorption.	352.89 mg/g	[42]
Tea industry waste (AC)	Aqueous solution	Phenol	30 mg of TWAC, with a pH adjusted to 6.0, agitated at 400 rpm for 4 hr	2-10	100-1000	0-500 min	20-200 g/L	0-40 °C	Film diffusion along with intraparticle diffusion	99.5%	[46]
Tea waste (magnetic particle-loaded tea waste)	Aqueous solutions	Seven different organic dyes	0.01 g MNLTW added to the 20 mL solution of different concentrations of dyes stirred for 35 min	2-9	20	5-50 min	0.01–0.05 g	25°C	Physical and chemical adsorption.	126.58 mg/g, 87.72 mg/g, 82.64 mg/g, 129.87 mg/g, 119.05 mg/g, 113.64 mg/g, 128.21 mg/g for neutral red, reactive blue 19, Congo red, Janus green, crystal violet, and methylene blue, respectively.	[118]
Rice husk (AC)	Synthetic water	PAHs naphthalene (NA), phenanthrene (PH), pyrene (PY)	Adsorption test conducted at 200 rpm (28 ± 1°C)		0.25-3.5	1 to 7 d	0.1–7 mg	25, 35, and 45°C	Intraparticle diffusion	63.6 mg/g, 50.4 mg/g, 104.5 mg/g for NA, PH, and PY, respectively.	[47]
Nickel sulfide nanoparticles loaded on AC	Synthetic water	Methylene blue (MB) and safranin-O	0.005–0.025 g of adsorbent was added in 50 mL beakers on magnetic stirrer (750 rpm)	1-11	5–25	2–34 min	0.005-0.025 g	25°C	Adsorption	99.9%	[69]
Tea waste (BC)	Solution	Sulfamethazine (SMT)	Adsorbent dose of 1 g/L was added at 25°C in shaker (100 rpm) for 72 hr	3-9	0-50	—	1 g/L	25°C	The π-π electron donor–acceptor interaction	33.81 mg/g	[10]
Tea waste (black tea and waste black or green tea)	Stock solutions	Methylene blue (MB) and eosin yellow (EY)	Adsorbent mixed in 250 mL flask of dye solution and stirred at 100 rpm	3-11	200–400	0-360 min	1-3 g/L	303 K-313 K	Electrostatic attraction	97.5% for MB 96.6% for EY	[48]
Date stones	Stock solution	L-Phenylalanine	50 mg mass of adsorbent mixed with adsorbate solution (200 mg/L) at 150 rpm for 300 min	2-9	50-1000	0-330 min	50 mg	20, 25, 35, and 40°C	Hydrogen bonding formation, hydrophobic and electrostatic interactions	114 mg/g	[49]

Table 2: Continued.

Material	Sample	Pollutant	Adsorption batch study	pH	Initial conc. Of adsorbate (mg/L)	Contact time	Adsorbent dosage	Temp.	Adsorption mechanism	Max removal efficiency	Ref.
Municipal sewage sludge and tea waste	Aqueous solutions	Methylene blue (MB)	The solution was shaken at 180 rpm and 25°C for 1 day	2-11	100	24 h	2 -50 g/L	25, 35, and 45°C	Electrostatic interaction, ion exchange, surface complexation, physical function	100%	[60]
Magnetic nanoparticle	Aqueous solutions	Cd^{2+} and acenaphthene	Adsorbent was mixed with 20 mL of adsorbate solution (1 mg/L) and placed on shaker by using vials	4-10	0.5-50	0-6 hr	0.25-1.25 g/L	22-25°C	Hydrophobic reactions for acenaphthene Complexation reaction for Cd^{2+}	2250 mg/kg and 1060 mg/kg for Cd^{2+} and acenaphthene, respectively	[92]
Tea waste and rice husk (BC)	Aqueous solutions	Carbofuran	1 g/L BC added into 50 mg/L solution of carbofuran and shaken at 100 rpm (30°C)	5	5-100	5-500 min	1 g/L	25, 35, and 45°C	Pore diffusion, π-π interaction, H-bonding, van der Waals forces, and chemical bindings	22.3 and 6.9 mg/g on TWBC and RHBC, respectively	[15]
Cornstalk nZVI/BC Cornstalk BC500 BC600 BC700	Aqueous solutions	Trichloroethylene (TCE)	30 mg/L TCE solution was treated with BC at 250 rpm	6.25, 7, and 8	30	—	100 mg	25°C	Partition and adsorption.	99% 93.28%, 91.33%, and 91.74%, respectively	[119]
Enteromorpha prolifera	Aqueous solution	Pyrene (PYR) and benzo(a)pyrene (BAP)	100 mL of PYR (50 μg/L) and BAP (20 μg/L) solutions with 0.05 g BC dosage were shaken at 150 rpm for 24 hr	2, 4, 7, 10, and 12	10-150 μg/L for PYR 10-60 μg/L for BAP	0-600 min	0.01-0.1 g	25°C	Chemical adsorption	187.27 μg/g and 80.00 μg/g for PYR and BAP, respectively	[62]
Dewatered sewage sludge	Stock solution	Phosphate	At 25°C, 0.12 g modified BC added in phenol solution (100 mL, 50 mg/L) at pH 4.5 and shaken for 3 hr	3-12	25, 50, 75, 100, 125, 150, and 175	10, 25, 40, 60, 90, 120, 150, and 180 min	1-2.6 g/L	25, 35, and 45°C	Electrostatic attraction	96.8%	[39]

Table 2: Continued.

Material	Sample	Pollutant	Adsorption batch study	pH	Initial conc. Of adsorbate (mg/L)	Contact time	Adsorbent dosage	Temp.	Adsorption mechanism	Max removal efficiency	Ref.
Tea waste	Stock solutions	Nitrate	Adsorbate solution with TW adsorbent placed in vapor bath constant temperature vibrator at 25 ± 2°C at 300 rpm for 120 min	1-12	25–1500	1–300 min	1–32 g/L	25 ± 2 °C	Electrostatic attraction, ion exchange	Max. ads. =132.26 mg/g, 89.2%, pH =3-10, dosage =8 g/L	[108]
		Phosphate		1-12	50–800	1–300 min	0.4–3.6 g/L	25 ± 2 °C	Electrostatic attraction, ion exchange	99.51 mg/g, 92.3%	

that for 100 mg/L initial concentration of MB, pH = 9.5, and temperature of 25°C, the optimum adsorption potential of AC-alginate was achieved as 230 mg/g. Maazinejad et al. [74] found that the initial concentration of MB dye was the most significant factor in adsorption of the dye by single-walled carbon nanotubes functionalized with an amine group (SWCNT-NH_2).

3.1.2. Chemical Oxygen Demand (COD). Chemical Oxygen Demand (COD) is an estimate of organic pollutants in wastewater relevant to the design and assessment of processes for biological treatment (Khairalla and Lu-Xiwu, [75]; [76]). It refers to the amount of oxygen required to oxidize organic compounds to carbon dioxide, ammonia, and water and is used as one of the main parameters of water quality in wastewater treatment plants [77]. COD is not only produced by organic compounds but also by some inorganic compounds [78]. Primary treatment of wastewater decreases about 27% of the influent COD, and downstream units are expected to further reduce COD concentration to satisfy indirect or direct discharge limits.

Activated carbon is used in both powder (PAC) and granular (GAC) forms with typical particle sizes between 15-25 μm and 0.2–5 mm in landfill leachate treatment schemes [79]. Pecan shell-based AC was used for the treatment of COD in municipal wastewater [45]. Various activation methods were employed, e.g., steam, acid, and carbon dioxide activation methods. Among all the carbons, steam and acid-activated carbons produced the largest surface areas of about 917 and 904 m^2/g, respectively. Adsorption was found highly dependent on the surface area of the carbons. Halim et al. [80] conducted an adsorption study for removal of COD in landfill leachate with an initial concentration of 2580 mg/L. Adsorption of 93.7% was obtained after generation of zeolite-activated carbon (Z-C) composite adsorbent. Combination of AC and zeolite in composite media acted as a natural ion exchanger and provided both hydrophobic and hydrophilic surfaces for the removal of organic (COD) and inorganic (ammonia) pollutants [81]. Devi et al. [82] studied the removal of COD concentration with avocado peel-activated carbon (APC) and compared with commercial activated carbon (CAC). The optimal operating conditions for maximum reduction of COD were also determined in the study. It was found that under ideal operating conditions using APC, the maximum percentage reduction in COD concentration was 98.20% and this reduction was 99.02% with CAC. Mohan et al. [83] investigated the adsorption efficiency of various ACs prepared from coconut shell fiber (CSF), coconut shell (CS), and rice husk (RH) for removal of COD from industrial wastewater. The removal efficiency obtained was 47-72% by CSFAC, 50-74% by CSAC, and 45-73% by RHAC. El-Naas et al. [32] reported that COD adsorption efficiency of date pit AC was comparable to commercially available AC when applied to petroleum refinery wastewater. The optimum values of AC dosage, contact time, and temperature were reported as 20 g/L, 30 min, and 60°C, respectively, whereas it was found out that the initial pH of wastewater had no significant impact on the removal efficiency of COD. The COD removal efficiency obtained at optimum conditions was 241.45 mg/g using the date pit AC.

3.1.3. Polycyclic Aromatic Hydrocarbons (PAHs). Polycyclic aromatic hydrocarbons (PAHs) are organic pollutants containing rings of carbon and hydrogen atoms such as naphthalene, phenanthrene, fluorene, anthracene, and pyrene [84]. They are identified as priority pollutants and are dispersed into the water by incomplete burning of fossil fuels [85]. PAHs are receiving attention because of their carcinogenicity, teratogenicity, and mutagenicity. They are highly lipophilic and carry toxicological effects on both aquatic organisms and humans via food chains [86]. Based on their molecular weight, PAHs are classified into two classes: low molecular weight PAHs emitted to the atmosphere and high molecular weight PAHs that stay in the water or settle to the bottom of water bodies [87]. PAHs have been found to be hydrophobic in nature; nonpolar and hydrophobic adsorbents show high adsorption efficiency for PAHs [88].

Yakout et al. [47] correlated hydrophobicity coefficient ($\ln K_{ow}$) with adsorption rate of hydrophobic PAHs (naphthalene, phenanthrene, and pyrene) onto rice husk-produced AC. A good correlation was found and increase in the coefficient and adsorption rate K (mg/g/$h^{1/2}$) were parallel using Weber-Morris equation. Zhang et al. [89] found that the rise in salinity resulted in an improvement in the rate of naphthalene elimination but had scarce effect on phenanthrene and pyrene removal. The findings revealed that the adsorptive equilibrium capacities of naphthalene, phenanthrene and pyrene on the U detritus were 1.27, 1.97, and 2.49 mg/kg, respectively, at the initial concentration of 10 μg/L. Kumar et al. [90] investigated the efficiency of PAH removal using palm shell AC. The AC was further modified by 5% KOH and thermal treatment. It was found that thermally modified KOH-soaked AC had superior adsorption capability of 131.1 mg/g for PAHs, whereas initial concentration of the pollutant was an important factor in controlling the process efficiency. Another study reported adsorptive removal of six PAHs, viz., naphthalene, acenaphthene, fluorene, anthracene, pyrene, and fluoranthene, as 145, 111, 145, 232, 109, and 93 g/kg using granular AC [91]. Pore diffusion was found as a prominent mechanism of adsorption onto AC. The reported values were higher than other reported values in literature. When heavy metals and organic compounds exist side by side, they are expected to interfere and therefore have a synergetic impact on human health and other species [56]. Huang et al. [92] synthesized magnetic nanoparticle adsorbents to simultaneously extract polycyclic aromatic hydrocarbons (acenaphthene) and metal pollutants (Cd^{2+}). The adsorption capacity was up to 1060 mg/kg and 2250 mg/kg for acenaphthene and Cd^{2+}, respectively. It was observed that the sorption capability decreased compared with the individual sorption, suggesting competitive sorption between both adsorbates, but the efficiency of simultaneous sorption was stable over a broad pH spectrum as well as in the presence of competing metal ions or natural organic matter.

3.1.4. Pharmaceuticals. The presence of chemical drugs in aquatic ecosystems has been regarded as one of the major environmental concerns over the past decades. Effluents from municipal wastewater treatment plants have been shown to be the primary cause of pharmaceuticals in aquatic ecosystems. These pollutants may be degraded utilizing different specialized methods of oxidation, such as Fenton, Photo-Fenton, Fenton-like, and electrochemical oxidation. Such approaches have a high effectiveness of elimination for contaminants, but high energy and chemical demands are the main economic restrictions for advanced oxidation processes. Adsorption has been effectively used for the removal of drugs in literature. An antipsychotic drug, carbamazepine (CBZ), is one of the most recorded micropollutants in surface waters. Magnetite AC was used for the removal of CBZ from municipal wastewater, and 93% (182.9 mg/g) removal was achieved using 1 : 8 magnetite content and AC [27]. L-Phenylalanine, identical to other amino acids, is important to animals and to the human body. This is commonly used in food or feed additives, in infusion products and in nutraceutical and medicinal applications. In a study by Belhamdi et al. [49], porous AC was effectively synthesized from date stones, using the chemical activation process. The findings revealed that optimum factors, affecting the adsorption of L-phenylalanine, were temperature range of 20 to 40°C and pH of 2–9.4, with maximum adsorption capacity of 188.3 mg/g by KOH-modified AC.

Sodium diclofenac (SD) is used for the therapy of arthritis and is a commonly found pharmaceutical in aquatic environments. It is a sodium salt form of a derivative of benzene acetic acid and is persistent in nature. Malhotra et al. [50] reported that $ZnCl_2$-modified AC had the highest adsorption potential (62 mg/g) for SD in comparison to KOH- (49.5 mg/g) and K_2CO_3- (52.4 mg/g) modified AC. Phenol is a very toxic chemical produced by coal purification, paper, pulp, fertilizer, paint, and organic synthesis industries. They can also be transmitted by plants as natural resources. Phenolic compounds are strong irritants for skin and eyes. In most cases, they can cause death of living cells. Phenols can be removed effectively using adsorption method. Particularly, AC as an adsorbent has shown high removal efficiency for phenols due to its large and highly active surface area [46]. Magnetic carbonaceous materials (AC and BC) effectively removed phenol from water samples [93]. Magnetic alteration improved the AC's surface and pore capacity and retained biochar's structural properties. It was observed that magnetic AC had lower adsorption rate (10.641 g/mg/min) than virgin AC (20.575 g/mg/min), whereas magnetic BC had a higher adsorption rate (0.618 g/mg/min) compared to virgin BC (0.040 g/mg/min). Yang et al. [94] developed stable supramolecular gel adsorbent to solve the problem of recyclability. The absorbents in the gel were successful in extracting bicyclic phenols from aqueous solution. Lim et al. [95] reported the synthesis of novel polyvinyl alcohol cryogel beads with an exterior surface protected by powdered AC. The purpose was to shield the trapped activated sludge biomass from the inhibitory impact of the recalcitrant pollutant 4-chlorophenol. The powder AC dispersed on the outer surface of cryogel beads was shown to have a higher 4-chlorophenol adsorption potential than the homogenized powder AC beads. Overall, the elimination of 4-chlorophenol was achieved via the combined adsorption and biodegradation processes. Maximum 132 mg/g adsorption capacity was obtained using the material for 4-chlorophenol.

3.2. Biochar. Biochar has been used widely to remedy the deterioration of wastewater from organic contaminants. Many considerations, such as the types of feedstock, the dosage applied, the desired contaminants, and their concentration, have influenced the elimination of organic pollutants from wastewater by BC. In general, there is a higher affinity for adsorption of polar and ionic organic compounds on the polar BCs and a lower affinity for hydrophobic compounds. Application of BC for adsorption of various organic pollutants is discussed further.

3.2.1. Chemical Dyes. Fan et al. [60] developed biochar at 300°C by copyrolysis of waste from municipal sludge and tea waste with 53.21% yield. Up to 100% of MB removal was achieved by application of the BC for more than 24 h contact time and 100 mg/L initial concentration of adsorbent. The mechanisms of MB removal included electrostatic activity, exchanging of ions, complexation of the surface, and physical process. Huff and Lee [61] revealed that a higher percentage of H_2O_2 treatment with pinewood biomass BC contributed to a higher cation exchange capacity (CEC) due to the introduction of acidic oxygen functional groups on the BC surface. It also led to the subsequent reduction of the BC's pH while MB adsorption decreased with higher concentration of H_2O_2 treatments due to lowering of π-π dispersive forces. Methylene blue (MB), orange G (OG), and Congo red (CR) dye removal was studied using biochar prepared at very high temperature (900°C) [96]. Adsorption of 196.1 mg/g, 38.2 mg/g, and 22.6 mg/g was achieved for the three dyes, respectively. The adsorption was attributed to intraparticle diffusion, high surface area, and electrostatic interaction.

3.2.2. Chemical Oxygen Demand (COD). Adsorptive removal of total and dissolved COD was investigated by Huggins et al. [97] in brewery wastewater using granular biochar. Results revealed that BC had higher adsorption capacity for total COD as compared to dissolved COD. High adsorptive removal of total COD was attributed to removal of higher content of total suspended solids (TSS) due to macrostructure of BC, whereas in the case of dissolved COD, the TSS were filtered out and adsorptive removal was reduced. The results of COD removal were compared with granular AC (GAC). It was observed that adsorptive removal of total COD at 1200 mg/L initial concentration using BC (70 mg/g) was 30% higher compared to GAC (49.3 mg/g), whereas at lower initial concentrations and for dissolved COD, the adsorptive removal using BC was lower and almost like GAC. Manyuchi et al. [98] reported a reduction of 90% COD when the sewage wastewater was subjected to the urban sewage sludge BC. The sewage pH also shifted from alkaline to acidic after treatment. The findings suggested that

BC sewage sludge effectively treated the sewage wastewater. Khalil et al. [99] investigated the effect of pH, COD concentration, temperature, contact time, and the amount of adsorbent dosage on the removal of COD from aqueous solution by biochar obtained from rice straw. It was observed that the removal efficiency of COD increased with increasing initial concentration of COD, which was attributed to higher physical adsorption onto BC. The removal efficiency also improved with increasing pH from 2 to 8.5. A direct correlation was found between the BC dosage, temperature, and adsorption efficiency. The results demonstrated the maximum removal efficiency of COD of 90.44% from aqueous solutions at optimum conditions.

3.2.3. Polycyclic Aromatic Hydrocarbons (PAHs). Biochar have a smaller surface area than AC, but they can lessen the bioavailability of PAHs, pesticides, and heavy metals efficiently [100]. Yang et al. [101] investigated the adsorption of aromatic organic compounds onto various biochar prepared at high temperature (700°C). It was found that basic mechanisms involved in the adsorption of aromatic compounds were π-π interaction, hydrogen bonding, and hydrophobic effect. Pyrolysis is unable to fully carbonize the BC and thus forms both carbonized and amorphous organic matter. Higher pyrolysis temperature may favor PAH adsorption because of higher content of carbonized organic matter. Carbonized organic matter has a more compact, aromatic, and nonpolar composition, including associations with planar and aromatic PAHs which are more beneficial in adsorption [102]. Godlewska et al. [103] reported that during pyrolysis switching from N_2 to CO_2 gas favored the adsorption of phenanthrene and pyrene onto BC. Increased adsorption was connected to the higher aromatic nature of BC prepared by the former gas. Biochar prepared from municipal waste was found to be a reliable and recyclable adsorbent for PAHs, phenols, and petroleum-based materials in aqueous media [104]. Macroaglae (Enteromorpha prolifera and Ulva lactuca) BC and modified BC (by ferric and zinc chloride) was reported by Cheng et al. [105] for adsorption of PAHs particularly naphthalene (NAP), acenaphthene (ACE), and phenanthrene (PHE). Adsorption capacity of about 90 mg/g was achieved by pore filling and π-π interaction following Freundlich adsorption model and showing heterogeneous adsorption for all pollutants on the BC. This value was higher than other reported values of adsorption, e.g., mangrove litter BC, 47.27 mg/g for 3-ring PAHs, 66.01 mg/g for 4-ring PAHs, and Phragmites australis BC (1.97 mg/g) for PHE [106].

3.2.4. Pharmaceuticals. Carbofuran (a pesticide) was removed from the aqueous solution by rice husk and tea waste BC produced at 700°C [15]. The equilibrium adsorption potential calculated by the pseudo-second-order kinetic model was 25.2 and 10.2 mg/g for rice husk and tea waste BC, respectively. It showed that carbofuran adsorption on rice husk biochar was 2.5 times higher than that on tea waste. 95% of carbamazepine (CBZ), a famous pharmaceutical, was removed using nano-BC (60 nm particle size) prepared from pinewood residue material [107]. The prepared BC showed a good removal efficiency (up to 57%) for CBZ in the presence of surfactant (Tween 80) as well.

Phosphorus is an important resource in modern agricultural development and pharmaceutical processing. Large amounts of nitrates and phosphates in water threaten the biological equilibrium of the system and exacerbate the water quality. Excessive phosphorous release promotes the uncontrolled development of bacteria and algae (eutrophication) that compete in the water with fish and aquatic insects for dissolved oxygen and deteriorate the aquatic environment [39]. Qiao et al. [108] prepared a low-cost and highly efficient biosorbent prepared by tea waste and modified by amine crosslinking and tested for its ability to remove phosphate and nitrate ions from aqueous solutions. It was observed that the material had limited nitrate and phosphate adsorption capability before modification. Amine-crosslinked biosorbent had 136.43 mg/g and 98.72 mg/g nitrate and phosphate adsorption capability, respectively, over a wide pH range.

Wan et al. [109] focused on the optimal conditions for preparation of the eucalyptus sawdust biochar as a possible biosorbent of nitroimidazoles from aqueous solutions. The activation temperature and H_3PO_4-to-sawdust impregnation ratio were significant factors in maximizing metronidazole's adsorption capacity. The optimally formulated biochar removal efficiencies were 97.1% and 96.4% for metronidazole and dimetridazole at 20 mg/L concentration and 1.0 g/L dosage within 2 h, respectively, while the thermodynamic analysis showed spontaneity and exothermicity in the adsorption process. Tetracyclines (TCs) are rated as second antibiotics used worldwide and are mostly released in unchanged form in the environment due to poor metabolization. Chen et al. [110] studied adsorption of TCs onto H_3PO_4-modified animal manure and rice husk BCs. According to isothermal study, the latter showed higher removal efficiency as compared to the animal manure BC with capacity of 552 mg/g and 365.4 mg/g, respectively. However, the maximum adsorption value was higher than other reported values in literature, i.e., alkali BC (58.8 mg/g) [111], NaOH-modified BC (455.33 mg/g) [112], Pinus taeda-activated BC (274.8 mg/g) [113], wood BC (96.1 mg/g) [114], and cobalt-impregnated BC (370.37 mg/g) [115]. Simultaneous removal of norfloxacin, sulfamerazine, and oxytetracycline was studied using KOH-modified BC (Luo et al., [116]). It was observed that in ternary-solute, the sorption kinetics of the three antibiotics were faster than that of the single-solute unit and the process was controlled by BC electrostatic interactions, π-π interaction, and H-bonding. The new BC-supported magnetic CuZn-Fe_2O_4 composite (CZF–biochar) was formulated through a simple hydrothermal method by Heo et al. [117] to extract bisphenol A (BPA) and sulfamethoxazole (SMX) from the aqueous media. The key pathways for adsorption were H-bonding, hydrophobic, and π–π interactions with maximum monolayer adsorption capacity of about 263.2 mg/g and 212.8 mg/g for BPA and SMX, respectively.

4. Adsorption Models

Various models are used to understand and describe the adsorption mechanism. The models are discussed as follows.

4.1. Adsorption Isotherm Models. Isotherm experiments are conducted to obtain the relationship between adsorbate concentration, the amount of adsorbate adsorbed, and the amount of adsorbent at equilibrium. Isotherms play a major function when considering the statistical models for the design and study of adsorption processes. The experimental results obtained in a specific study under one collection of conditions may fail under another. To evaluate the correct fit model for the adsorption process, error analysis involves the use of root mean square error, chi-square, and average relative error. If the value of error measurements is small, the experimental and measured results are more comparable by isothermal and kinetic methods; if they are large, the value would be higher [120]. Table 3 shows that mostly adsorption by carbonaceous materials can be expressed by Langmuir and Freundlich models, and various parameters help in understanding the mechanism. Some common isotherm models are discussed as follows.

The Langmuir model is based on the hypothesis that adsorption happens inside the adsorbent at different homogeneous locations, and there is no substantial interference between the adsorbates [36]. The adsorbate is saturated at the adsorbent surface after one layer (mono layer) of adsorbed molecules is formed [120]. The linearized version of the Langmuir equation is as follows [121]:

$$\frac{C_e}{q_e} = \frac{1}{K_L q_m} + \frac{C_e}{q_m}, \tag{3}$$

where q_e is the mass of adsorbate on the surface of the adsorbent (mg/g) at equilibrium, C_e is the equilibrium adsorbate concentration in solution (mg/L), q_m is the maximum adsorption power (mg/g), and K_L is the Langmuir adsorption constant (L/mg). Linearized forms of isotherm models are commonly reported in most studies. The dimensionless constant R_L, originating from the Langmuir model, is named as the separation factor or equilibrium parameter [16].

$$R_L = 1 + \frac{1}{K_L C_0}. \tag{4}$$

R_L values signify isotherm forms which are either unfavorable ($R_L > 1$), linear ($R_L = 1$), desirable ($0 < R_L < 1$), or irreversible ($R_L = 0$) [122].

The Freundlich isotherm is a variational sorption model. It suggests monolayer sorption with a heterogeneous energy distribution of active sites, followed by encounters between adsorbed molecules [123]. Linear form of the model is as follows [124]:

$$\log q_e = \log K_F + \frac{1}{n} \log C_e, \tag{5}$$

where q_e is the mass of adsorbate, at equilibrium, on the surface of the adsorbent (mg/g); C_e is the equilibrium adsorbate concentration in solution (mg/L); K_F is the Freundlich adsorption constant, which implies the adsorption efficiency; and n is the nonlinearity measurement. The value of $1/n$ less than 1 shows the physical adsorption phenomena and favors the adsorption process (Liu et al., [125]).

The Temkin isotherm model is being studied because of the potential adsorption heat interaction. This model suggests that bond energies are defined by a standardized distribution of the molecular adsorption energy. This would mean that the adsorption heat of the molecules present in the surface layer would be reduced linearly with the coverage [126]. The linear form of the Temkin model is given as follows:

$$q_e = \frac{RT}{b_T} \ln (K_T) + \frac{RT}{b_T} \ln (C_e), \tag{6}$$

where R is the ideal constant for gases, 8.314 J/mole K; T is the adsorption temperature, K; b_T is the adsorption heat constant, J/mol; and K_T is the Temkin isotherm constant, L/g.

The Dubinin–Radushkevich (D-R) isotherm model is generally used to determine the adsorption mechanism on a heterogeneous surface with a Gaussian energy scattering. The model is well adapted to strongly active solutes and low concentrations. While the D–R isotherm model is also regarded as parallel to the Langmuir isotherm model, it does not consider the possibility for homogeneous surface or persistent adsorption [52]. The linear form of the D-R model is given as follows:

$$\ln (q_e) = \ln (q_m) - \beta\varepsilon^2, \tag{7}$$

where q_e (mol/L) and q_m (mol/g) are the sum of the adsorption per unit weight and the peak adsorption potential, respectively. The parameter β ($\text{mol}^2 \cdot \text{J}^{-2}$) is the coefficient of activity depending on the mean adsorption free energy and ε ($\text{RT} \ln (1 + 1/C_e)$) is the Polanyi potential.

4.1.1. Isotherm Types. According to the international union of pure and applied chemistry (IUPAC), the equilibrium of physical adsorption process has different adsorption isotherms that may be categorized as type I to type VI [127]. These isotherms help to understand the multiple adsorption processes including monomolecular, multimolecular adsorption, and condensation in pores or capillaries [128]. Figure 2 shows the classification of the isotherms and associated adsorption characteristics over a particular range of relative pressure (P/P_o) [129]. These isotherms have different patterns due to pore shape, adsorption process, and adsorbent/adsorbate interactions.

Type I isotherms have a very quick rise in adsorbed amount with increasing concentration (or pressure) up to saturation; i.e., they have a partially or completely horizontal plateau [130]. Microporous materials having a small portion of the outer surface are classified as this type. Such isotherms resemble Langmuir isotherms showing monolayer adsorption [131]. Polymolecular adsorption in nonporous or macroporous adsorbents is classified as Type II. It does not represent a saturation limit. Type III sorbents are nonporous and have a low adsorbent-adsorbate interaction energy. Types IV and V are porous adsorbents, which are

Table 3: Isothermal and kinetic models used in various adsorption studies.

Material	Adsorbent	Pollutant	Isotherm models	Fitting model	Model parameters	Kinetic models	Fitting model	Model parameters	Ref.
Pine wood sawdust	Charcoal	Phenanthrene, anthracene and pyrene (PAHs)	Polanyi–Dubinin–Manes (PDM) model and Freundlich	Freundlich	R^2=0.99	—	—	—	[139]
Oil palm shell	AC	Methylene blue (basic dye)	Langmuir, Freundlich, Temkin, and Dubinin–Radushkevich	Langmuir	q_m=243.9 mg/g, b=0.93 mg/L, R^2=0.99 at T=303 K	PFO, PSO, and IPDM	PSO	q_e=243.90 mg/g, k_2=0.005 g/mgh, R^2=0.99	[8]
Oil palm frond	AC	2,4-Dichlorophenoxyacetic acid	Langmuir and Freundlich	Langmuir	q_m=352.89 mg/g, K_L=0.013 L/mg, R^2=0.999 at 30 C	PFO and PSO	PSO	k_2=0.0224 g/mgh, q_e=157.98 mg/g, R^2=0.993	[42]
Coconut shells	AC	Hydrophobic organic compounds (HOCs), e.g., PAHs, polychlorinated biphenyls (PCBs)	Freundlich	Freundlich	$n = 1.05 \pm 0.03$, R^2=0.90±0.01 (for pyrene) $n = 1.22 \pm 0.20$, R^2=1.11±0.06 (for PCB)	—	—	—	[68]
Tea industry waste	AC	Phenol	Langmuir and Freundlich	Langmuir	q_m=142.9 mg/g, b=1.51 mg/L, $K_L = 1 * 10^{-2}$ L/mg, R^2=0.9967, R_L<1	PFO, PSO, and IPDM	PSO	—	[46]
Tea waste	Magnetic nanoparticle-loaded tea waste	Seven different organic dyes Janus green, methylene blue, thionine, crystal violet, Congo red, neutral red, and reactive blue 19	Langmuir, Freundlich, Sips, Redlich–Peterson, Brouers–Sotolongo, and Temkin	Langmuir model for all dyes	q_m=126.58 mg/g for NR, 129.87 mg/g for JG, 128.21 mg/g for TH, 113.64 mg/g for CV, 82.64 mg/g for CR, 119.05 mg/g for MB, 87.72 mg/g for RB	PFO and PSO	For cationic dyes, PSO, and for anionic dyes, PFO	For TH, K_2=0.007 g/mg/min, q_e=20 mg/g For MB, K_2=0.0121 g/mg/min, q_e=20 mg/g For CV, K_2=0.0111 g/mg/min, q_e=13.3 mg/g For JG, K_2=0.0169 g/mg/min, q_e=20 mg/g	[118]

Table 3: Continued.

Material	Adsorbent	Pollutant	Isotherm models	Fitting model	Model parameters	Kinetic models	Fitting model	Model parameters	Ref.
								For NR, K_2=0.0050 g/mg/min, q_e=20 mg/g For CR, K_1=0.0534/min, q_e=10 mg/g For RB, K_1=0.0806/min, q_e=10 mg/g	
Lightweight expanded clay aggregate	LECA	PAHs Phenanthrene, fluoranthene, and pyrene	Freundlich and Langmuir	Freundlich	K_F=0.22, 2.02, & 1.70; n = 1.48, 0.95, & 0.95; R^2=0.86, 0.97, & 0.92	—	—	—	[88]
Nickel sulfide nanoparticles loaded on activated carbon	NiS-NP-AC	Methylene blue and safranin-O	Langmuir, modified and nonmodified competitive Langmuir model, Langmuir-Freundlich, Freundlich and extended Freundlich	Langmuir	For MB, q_m=21.5 mg/g, K_L=1.76 L/mg, R^2=0.99 For SO, q_m=53.2 mg/g, K_L=0.231 L/mg, R^2=0.98	PFO, PSO, Elovich and intraparticle diffusion	PSO	For MB, K_2=66 g/mg/min, q_e=21.2 mg/g For SO, K_2=36 g/mg/min, q_e=33.6 mg/g	[69]
$Ti_3C_2T_x$		Dyes methylene blue (MB) and acid blue 80 (AB80)	Langmuir and Freundlich	Freundlich	n = 19.963 K_F=48.152 R^2=0.928	—	—	—	[140]
AC and iron salts	Magnetic AC	Carbamazepine	Langmuir, Freundlich, Dubinin–Radushkevich, Redlich-Peterson, Radke-Prausnitz, and Temkin	Radke-Prausnitz>Redlich-Peterson>Temkin>Freundlich>Langmuir>Dubinin-Radushkevich	$1/n_F$=0.31 K_L=0.743 L/mg	PFO, PSO, intraparticle diffusion, liquid film diffusion, and Elovich	Elovich>intraparticle diffusion>PSO>liquid film diffusion>PFO	K_2=8.70×10^{-3}, 1.47×10^{-2}, and 2.16×10^{-2} g/mg/min at 273, 288, and 303 K temperatures, respectively	[27]
Date stones	AC	L-Phenylalanine	Langmuir and Freundlich	Langmuir	R_L=0-1, q_m=188.3 mg/g	PFO and PSO	PSO	—	[49]

Table 3: Continued.

Material	Adsorbent	Pollutant	Isotherm models	Fitting model	Model parameters	Kinetic models	Fitting model	Model parameters	Ref.
Sewage sludge and tea waste	Biochar	Methylene blue	Langmuir, Freundlich, Temkin, Dubinin-Radushkevich (D-R)	Langmuir	q_m=19.3798 mg/g b=0.2871 mg/L R^2=0.9928	PFO, PSO, and Elovich equations	PSO	q_e=15.1745, K_2=0.001749 g/mg/min, at 45 C	[60]
Eggshell	AC	Dissolved hydrogen sulfide	Langmuir and Freundlich	Freundlich	q_m=289.3 mg/g	PFO and PSO	PSO	K_2=0.024 g/mg/min	[51]
Palm shell	Residual biomass	COD	Langmuir, Freundlich, and Temkin	Langmuir	b=0.0013 mg/L q_m=5.6380 mg/g R^2=0.99	PFO and PSO	PFO	q_e=2.8417 mg/g K_1=0.3652 g/mg/min R^2=0.9919	[126]
Sawdust	Residual biomass	COD	Langmuir, Freundlich, and Temkin	Langmuir	b=0.0033 mg/L q_m=32.7869 mg/g R^2=0.989	—	—	—	
Wood sawdust	AC	Hydrogen sulfide	Langmuir, Freundlich, Temkin, Dubinin–Radushkevich	Freundlich	K_F=9.57 mg/g $1/n$=1.40453 R^2=0.9926	—	—	—	[51]

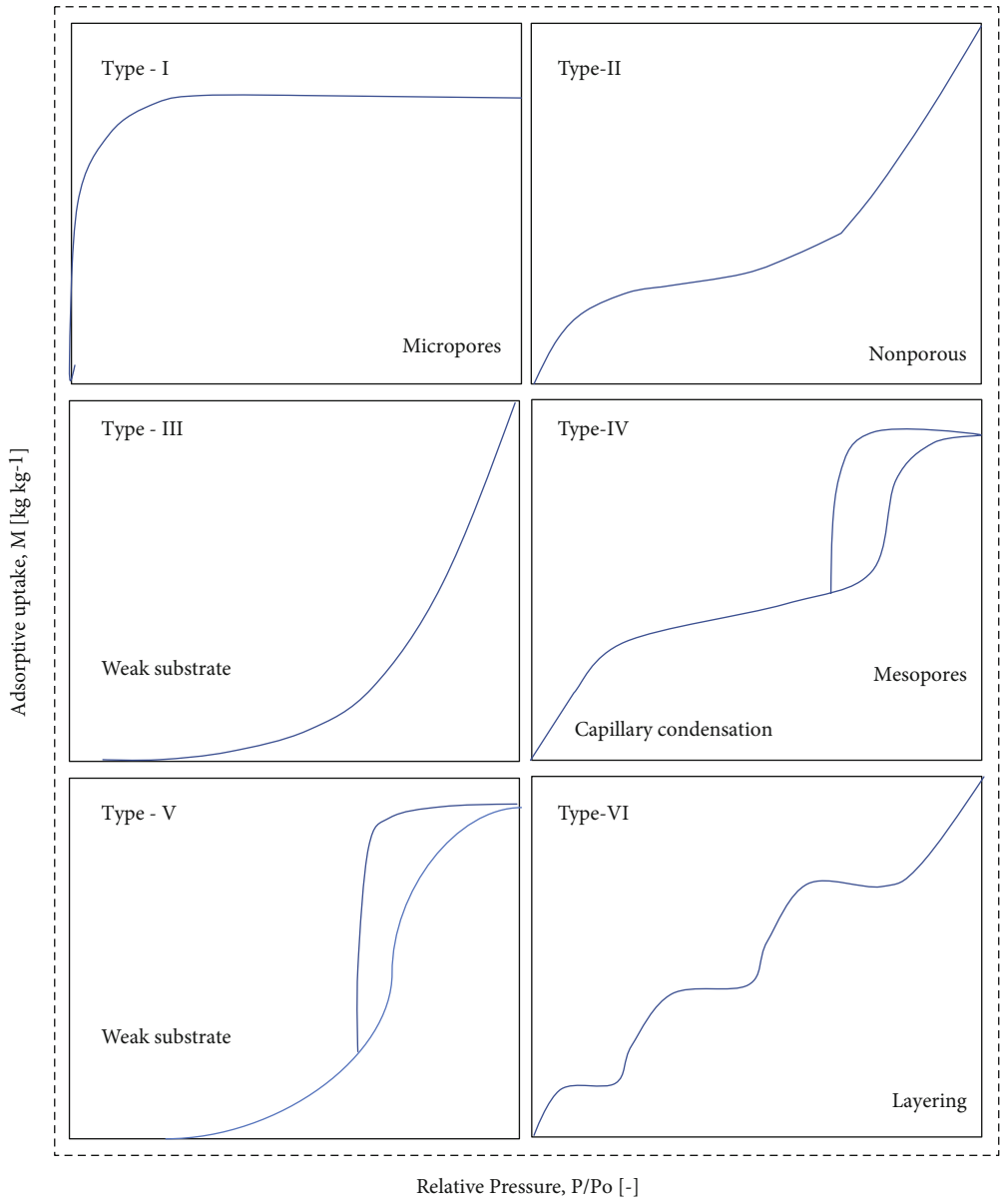

Figure 2: IUPAC classification of adsorption isotherms [129].

comparable to types II and III. This shows that a monolayer form first followed by a multilayer [132]. Nonporous adsorbents with a homogenous surface exhibit type VI isotherms. This isotherm is known as stepwise multilayer adsorption, and it only arises when the sample surface comprises many types of adsorption sites with energetically distinct properties [133].

4.2. Adsorption Kinetic Models. The impact of contact time is investigated to determine the possible application and to gain insight into adsorption kinetics. Generally, the adsorption process initially shows accelerated patterns, which can be due to surface complexation or instant electron transfer. Afterwards, the adsorption seems constant showing the gradual saturation of adsorption sites on the outside surface or reduced efficiency of redox processes [134]. The kinetic adsorption models are typically complex. The rate of adsorption is highly affected by many variables relevant to the solid state and the physical and chemical parameters by which the adsorption takes place [69]. To fully understand the kinetics of adsorption, four widely used kinetic models are pseudo-first-order (PFO), pseudo-second-order (PSO), Elovich, and intraparticle diffusion (ID) models [135]. Table 3 shows that most carbonaceous materials fit either the PFO or the PSO model for describing their adsorption mechanism. However, diffusional results can be very significant for porous sorbent materials, and therefore, the rate constants assessed by diffusion models must be calculated in order to obtain insight into the transfer mechanism.

The best fitting of experimental results to the pseudo-first-order (PFO) model suggests that adsorption to be more inclined towards physisorption interactions and that the

mechanism of adsorption depends on the initial adsorbate concentration [15]. The model equation is given as follows:

$$\ln (q_e - q_t) = \ln q_e - K_1 t, \tag{8}$$

where q_e (mg/g) and q_t (mg/g) are the amounts of adsorbed ions per unit mass of the adsorbent at equilibrium and at any time (t), respectively, and K_1 is the PFO model rate constant.

The pseudo-second-order (PSO) model relies on the hypothesis that chemical sorption such as bonding forces by sharing or the exchange of ions/electrons between adsorbate and adsorbent governs the phase reaction rate [16]. The model can be represented through the following equation:

$$\frac{t}{q_t} = \frac{1}{K_2 q_e^2} + \frac{1}{q_e} t, \tag{9}$$

where q_e (mg/g) and q_t (mg/g) are the amounts of adsorbed ions per unit mass of the adsorbent at equilibrium and at any time (t), respectively, K_2 is the PSO model rate constant. Adsorption rate constants and adsorption percentage may be different for various pollutants because the rate determines the diffusion of pollutants from water sample to solid adsorbent surface [136]. Khan et al. [137] found the inverse relation between K_2 and initial concentration of Cu(II) while q_e was directly related to the initial concentration.

The Elovich equation is often widely used to explain the kinetic second order given that the real solid surfaces are vigorously heterogeneous, but the method does not suggest any specific adsorbate-adsorbent mechanism [44]. It has been widely agreed that this semi-empirical equation can explain the chemisorption cycle. One may measure the Elovich coefficient from the plot, q_t versus $\ln t$. The early adsorption rate, a_e, and the desorption coefficient can be calculated from the interception and slope of the $q_t - \ln t$. The linear form of the equation is given as follows:

$$q_t = \frac{\ln (a_e b_e)}{b_e} + \frac{1}{b_e} \ln (t), \tag{10}$$

where a_e is the initial adsorption rate (mg/g/min) and b_e is the desorption constant (g/mg), which is related to the extent of surface coverage and activation energy for chemisorption.

Adsorption mechanism for understanding the diffusion process may be analyzed in terms of the intraparticle diffusion model, interparticle diffusion model, or Boyd's film diffusion model. According to the Weber and Morris model intraparticle diffusion model, if a linear curve is obtained and it passes through the origin, then the predominant mechanism for adsorption is diffusion. According to this model, an internal diffusion cycle regulates the adsorption capacity [52].

$$q_t = K_i t^{1/2} + C, \tag{11}$$

where q_t (mg/g) is the amount of adsorbed ions per unit mass of the adsorbent at any time (t), K_i is the rate of intraparticle diffusion, and C is a constant. The values of K_i and C are obtained from a plot of q_t versus time $t^{1/2}$. The multilinearity of the plot would indicate that more than one form of adsorption existed while adsorbing the adsorbents [138].

4.3. Adsorption Thermodynamics. The adsorption process's dependency on temperature can be clarified by thermodynamic analysis of the equilibrium results. In adsorption thermodynamics, the adsorption's spontaneity, thermochemical complexity, and randomness trend with respect to the temperature is correlated by the measurement of certain thermodynamic parameters, like Gibbs free energy change (ΔG°), enthalpy (ΔH°), and entropy (ΔS°). Among these parameters ΔG° is the key indicator used in confirming spontaneity of the adsorption process, and a negative ΔG° value implies that the adsorption process is spontaneous and feasible. The positive value of ΔH^o indicates that the process is endothermic. Positive value of ΔS^o shows affinity of the adsorbent for the adsorbate. These parameters can be calculated as follows [57]:

$$\Delta G^o = -RT \ln (K_c), \tag{12}$$

$$\Delta G^o = \Delta H^o - T\Delta S^o, \tag{13}$$

where $K_c = C_a/C_e$, C_a represents adsorbate per unit adsorbent mass (mg/g), C_e is the equilibrium adsorbent concentration in aqueous liquid (mg/L), and K_c is the equilibrium constant for adsorption; R is the uniform gas constant (8.314 J/mol/K) and T is the absolute temperature (K).

5. Adsorption Mechanism

In general, an adsorbent's adsorption capability depends basically on its physicochemical properties [141]. Adsorption may take place due to physical, chemical, or both physical and chemical reactions on the surface of the adsorbents. Physical adsorption may be by porous structure (i.e., AC and BC) and chemical adsorption by surface functional groups (i.e., -OH, -COOH, C-O) or others depending on the material properties, surface treatment methods, and reduction sites [142]. Table 3 states the mechanisms of adsorption reported in various studies using AC and BC. Studies showed that organic compounds are usually sorbed onto the carbonaceous materials due to a surface interaction reaction. Other mechanisms, such as π-π bond activity and pore filling, have also been demonstrated to lead to increased sorption and decreased desorption of organic pollutants onto the ACs and BCs (Luo et al., 2018; [143]). Schematic diagram of adsorption mechanism for organic pollutants on AC and BC is shown in Figure 3.

Characterization and modelling techniques help in identifying the adsorption mechanism. The mechanism of adsorption can be better defined from an FTIR study. Prior to and after adsorption the adsorbent samples are prepared for infrared (IR) study. The dynamic nature of the adsorbent and presence of various functional groups are seen by the amount of adsorption peaks in the spectra [65]. Liu et al.

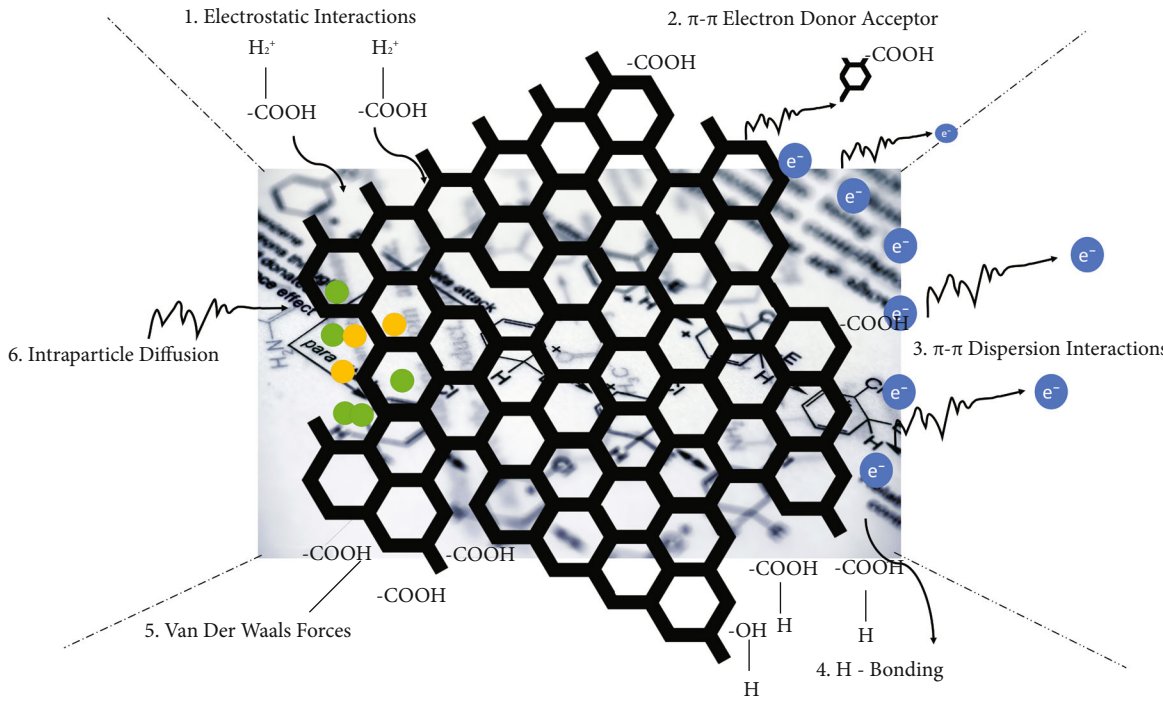

Figure 3: General adsorption mechanism of organic pollutants.

[144] found the inverse relationship between pyrolysis temperature (PT) and FTIR peaks assigned to -OH, C=C, and C=O groups and direct relationship between PT and peaks assigned to aromatic γ-CH. After adsorption, the peaks were reduced further, and complexation of functional groups was found as adsorption mechanism.

BET surface area analyzer helps in identifying the surface area and pore size variation before and after adsorption. The pore sizes may be micro (<2 nm), meso (2-50 nm), and macro (>50 nm) [145].

Type IV isotherm specifically shows that the substance being processed is of a mesoporous kind. In the adsorption isotherm, the relative pressure area shows the coexistence of micropores according to Henry's theorem [146]. There may be increase or decrease in surface area and pore size depending on the type of material. Decrease in pore size or specific surface area indicates the attachment or blockage of activating agent/pollutant at the surface of the adsorbent [147]. Increase in surface area indicates that surface pores opened up after modification/chemical activation [148].

XRD analysis shows the crystalline properties of adsorbents. It correlates the characteristic peaks with crystal planes in 2D representation (Zhang et al., [149]). Lee et al. [150] calculated the size of iron crystal in Fe_2O_3-carbon foam adsorbent as 38.32 nm using XRD analysis peak value. SEM, TEM, SEM-EDS, and TEM-EDS images of adsorbent materials help to know the surface morphology and elemental composition modification after adsorption [151]. Baghdadi et al. [27] observed large micropores and rough surface of nitric acid-treated AC after SEM analysis.

6. Conclusion

It has been observed that higher adsorption capacity, ease of generation, and relatively cheaper costs of carbon materials, e.g., ACs and BCs, have made them an attractive option for the removal of organic pollutants from wastewater. The preparation, modification, characterization, and application methods used for the adsorption of chemical dyes, COD, PAHs, and pharmaceuticals using AC and BC have been discussed in detail in this review. It was observed that in the majority of the studies, high pollutant removal efficiencies were reported using the adsorbents. Surface properties of the materials, e.g., pore size, surface area, pore diameter, and functional groups were found to be important factors in the adsorption process. The adsorption capacity also depends largely on the pyrolysis temperature, modification technique, initial pH of wastewater, dosage of material, contact time, and initial concentration of the pollutants. Parameters of the adsorption process and models used to understand the adsorption mechanisms have also been stated in the review. Characterization and simulation methods aid in the identification of the adsorption mechanism. Most of the studies concentrated on the kinetic, equilibrium, and thermodynamic aspects of adsorption, suggesting the dominant isotherm and kinetic models as Langmuir or Freundlich and pseudo-second-order models. Organic compounds are typically adsorbed on carbonaceous materials due to surface contact reactions such as bonding and pore filling. This review will help readers understand the current state of research in the adsorption of organic pollutants by agricultural waste-based ACs and BCs. However,

application of these adsorbents at the commercial scale has not been adequately investigated in research works and needs to be studied. Most of the studies have been conducted on synthetic solutions that do not completely represent the discharged effluents. This also needs attention in future studies.

7. Future Directions and Recommendations

The following are recommendations for future solid–liquid adsorption studies based on the review:

(i) There is a strong need for pilot and commercial scale application of adsorbents for removal of organic contaminants.

(ii) Research works need to be extended: on competitive adsorption studies of organic pollutants with other pollutant forms such as metals and other organics; also, there is need to demonstrate the molecular level analysis of the adsorbents to determine their main characteristics responsible for adsorption.

(iii) In addition, actual wastewaters should be investigated, rather than simulated wastewaters.

(iv) To minimize the expenses of the water treatment process, the combination of adsorption and other water management approaches should be explored.

Conflicts of Interest

The authors declare that they have no conflicts of interest.

Acknowledgments

The authors would like to acknowledge the financial support provided for this study under the YUTP grant with cost center 015LC0-190.

References

[1] A. M. Awad, R. Jalab, A. Benamor et al., "Adsorption of organic pollutants by nanomaterial-based adsorbents: an overview," *Journal of Molecular Liquids*, vol. 301, article 112335, 2020.

[2] I. Ali, M. Asim, and T. A. Khan, "Low cost adsorbents for the removal of organic pollutants from wastewater," *Journal of Environmental Management*, vol. 113, pp. 170–183, 2012.

[3] H. Khurshid, M. R. Mustafa, U. Rashid, M. H. Isa, Y. C. Ho, and M. M. Shah, "Adsorption study on DR28 dye by Subabul timber waste using Taguchi's laboratory test," *Environmental Technology & Innovation*, vol. 23, article 101563, 2019.

[4] E. H. Ezechi, M. H. Isa, S. R. M. Kutty, and A. Yaqub, "Boron removal from produced water using electrocoagulation," *Process Safety and Environmental Protection*, vol. 92, pp. 509–514, 2014.

[5] F. Piubeli, M. J. Grossman, F. Fantinatti-Garboggini, and L. R. Durrant, "Enhanced reduction of COD and aromatics in petroleum-produced water using indigenous microorganisms and nutrient addition," *International Biodeterioration and Biodegradation*, vol. 68, pp. 78–84, 2012.

[6] J. Wang and S. Wang, "Preparation, modification and environmental application of biochar: a review," *Journal of Cleaner Production*, vol. 227, pp. 1002–1022, 2019.

[7] S. Zhao, G. Huang, G. Cheng, Y. Wang, and H. Fu, "Hardness, COD and turbidity removals from produced water by electrocoagulation pretreatment prior to reverse osmosis membranes," *Desalination*, vol. 344, pp. 454–462, 2014.

[8] I. A. W. Tan, A. L. Ahmad, and B. H. Hameed, "Adsorption of basic dye using activated carbon prepared from oil palm shell: batch and fixed bed studies," *Desalination*, vol. 225, pp. 13–28, 2008.

[9] C. R. Altare, R. S. Bowman, L. E. Katz, K. A. Kinney, and E. J. Sullivan, "Regeneration and long-term stability of surfactant-modified zeolite for removal of volatile organic compounds from produced water," *Microporous and Mesoporous Materials*, vol. 105, pp. 305–316, 2007.

[10] A. U. Rajapaksha, M. Vithanage, M. Zhang et al., "Pyrolysis condition affected sulfamethazine sorption by tea waste biochars," *Bioresource Technology*, vol. 166, pp. 303–308, 2014.

[11] X. J. Lee, L. Y. Lee, S. Gan, S. Thangalazhy-Gopakumar, and H. K. Ng, "Biochar potential evaluation of palm oil wastes through slow pyrolysis: thermochemical characterization and pyrolytic kinetic studies," *Bioresource Technology*, vol. 236, pp. 155–163, 2017.

[12] R. Asadpour, N. B. Sapari, M. H. Isa, S. Kakooei, and K. U. Orji, "Acetylation of corn silk and its application for oil sorption," *Fibers and Polymers*, vol. 16, pp. 1830–1835, 2015.

[13] R. Asadpour, N. B. Sapari, M. H. Isa, and S. Kakooei, "Acetylation of oil palm empty fruit bunch fiber as an adsorbent for removal of crude oil," *Environmental Science and Pollution Research*, vol. 23, pp. 11740–11750, 2016.

[14] M. B. Desta, "Batch sorption experiments: Langmuir and Freundlich isotherm studies for the adsorption of textile metal ions onto teff straw (*Eragrostis tef*) agricultural waste," *Journal of Thermodynamics*, vol. 2013, Article ID 375830, 6 pages, 2013.

[15] M. Vithanage, S. S. Mayakaduwa, I. Herath, Y. S. Ok, and D. Mohan, "Kinetics, thermodynamics and mechanistic studies of carbofuran removal using biochars from tea waste and rice husks," *Chemosphere*, vol. 150, pp. 781–789, 2016.

[16] N. Zhou, H. Chen, Q. Feng et al., "Effect of phosphoric acid on the surface properties and Pb(II) adsorption mechanisms of hydrochars prepared from fresh banana peels," *Journal of Cleaner Production*, vol. 165, pp. 221–230, 2017.

[17] R. Gao, L. Xiang, H. Hu et al., "High-efficiency removal capacities and quantitative sorption mechanisms of Pb by oxidized rape straw biochars," *Science of the Total Environment*, vol. 699, article 134262, 2020.

[18] A. Nasrullah, A. H. Bhat, M. H. Isa et al., "Efficient removal of methylene blue dye using mangosteen peel waste: kinetics, isotherms and artificial neural network (ANN) modeling," *Desalination and Water Treatment*, vol. 86, pp. 191–202, 2017.

[19] M. B. Ahmed, J. L. Zhou, H. H. Ngo, W. Guo, and M. Chen, "Progress in the preparation and application of modified biochar for improved contaminant removal from water and wastewater," *Bioresource Technology*, vol. 214, pp. 836–851, 2016.

[20] A. O. Dada, A. P. Olalekan, A. M. Olatunya, and O. J. Dada, "Langmuir, Freundlich, Temkin and Dubinin–Radushkevich isotherms studies of equilibrium sorption of Zn^{2+} unto

phosphoric acid modified rice husk," *IOSR Journal of Applied Chemistry*, vol. 3, pp. 38–45, 2012.

[21] L. Zhang, W. Niu, J. Sun, and Q. Zhou, "Efficient removal of Cr(VI) from water by the uniform fiber ball loaded with polypyrrole: static adsorption, dynamic adsorption and mechanism studies," *Chemosphere*, vol. 248, article 126102, 2020.

[22] S. K. Sari, N. Trikurniadewi, S. N. Ibrahim, A. M. Khiftiyah, A. Z. Abidin, and T. Nurhariyati, "Bioconversion of agricultural waste hydrolysate from lignocellulolytic mold into biosurfactant by *Achromobacter* sp. BP (1)5," *Biocatalysis and Agricultural Biotechnology*, vol. 24, article 101534, 2020.

[23] K. K. Hammud, A. M. Raouf, A. Mohammed, A. Al-Sammarrie, and R. R. Neema, "FTIR, XRD, AFM, and SEM spechtroscopic studies of chemically MW-waste cooked tea activated carbon," *INTERNATIONAL JOURNAL OF RESEARCH IN PHARMACY AND CHEMISTRY*, vol. 6, no. 3, pp. 220–229, 2016.

[24] A. S. Ibrehem, "Experimental and theoretical study to optimize rate constants of adsorption and desorption of the wastewater treatment using waste of tea plant," *Arabian Journal for Science and Engineering*, vol. 44, pp. 7361–7370, 2019.

[25] A. Tapfuma, D. P. Chakawa, L. B. Moyo, N. Hlabangana, G. Danha, and E. Muzenda, "Investigating the feasibility of using agricultural waste as an adsorbent of gold ions in small scale gold processing plants," *Procedia Manufacturing*, vol. 35, pp. 85–90, 2019.

[26] P. Liu, C. J. Ptacek, D. W. Blowes, Y. Z. Finfrock, and Y. Y. Liu, "Characterization of chromium species and distribution during Cr(VI) removal by biochar using confocal micro-X-ray fluorescence redox mapping and X-ray absorption spectroscopy," *Environment International*, vol. 134, article 105216, 2020.

[27] M. Baghdadi, E. Ghaffari, and B. Aminzadeh, "Removal of carbamazepine from municipal wastewater effluent using optimally synthesized magnetic activated carbon: adsorption and sedimentation kinetic studies," *Journal of Environmental Chemical Engineering*, vol. 4, no. 3, pp. 3309–3321, 2016.

[28] R. Dhawan, M. Goyal, and K. K. Bhasin, "Influence of metal impregnants on adsorption of dimethylsulfide vapors by activated carbons," *Materials Today: Proceedings*, vol. 4, pp. 10515–10519, 2017.

[29] S. M. Kharrazi, N. Mirghaffari, M. M. Dastgerdi, and M. Soleimani, "A novel post-modification of powdered activated carbon prepared from lignocellulosic waste through thermal tension treatment to enhance the porosity and heavy metals adsorption," *Powder Technology*, vol. 366, pp. 358–368, 2020.

[30] L. Kong, Y. Gao, Q. Zhou, X. Zhao, and Z. Sun, "Biochar accelerates PAHs biodegradation in petroleum-polluted soil by biostimulation strategy," *Journal of Hazardous Materials*, vol. 343, pp. 276–284, 2018.

[31] R. Soysa, Y. S. Choi, S. J. Kim, and S. K. Choi, "Fast pyrolysis characteristics and kinetic study of Ceylon tea waste," *International Journal of Hydrogen Energy*, vol. 41, pp. 16436–16443, 2016.

[32] M. H. El-Naas, S. Al-Zuhair, and M. A. Alhaija, "Reduction of COD in refinery wastewater through adsorption on date-pit activated carbon," *Journal of Hazardous Materials*, vol. 173, no. 1–3, pp. 750–757, 2010.

[33] K. Jindo and T. Sonoki, "Comparative assessment of biochar stability using multiple indicators," *Agronomy*, vol. 9, pp. 1–11, 2019.

[34] H. A. H. I. Amarasinghe, S. K. Gunathilake, and A. K. Karunarathna, "Ascertaining of optimum pyrolysis conditions in producing refuse tea biochar as a soil amendment," *Procedia Food Science*, vol. 6, pp. 97–102, 2016.

[35] A. Cibati, B. Foereid, A. Bissessur, and S. Hapca, "Assessment of *Miscanthus* × *giganteus* derived biochar as copper and zinc adsorbent: study of the effect of pyrolysis temperature, pH and hydrogen peroxide modification," *Journal of Cleaner Production*, vol. 162, pp. 1285–1296, 2017.

[36] X. Yin, X. Yin, P. Shao et al., "Protonation of rhodanine polymers for enhancing the capture and recovery of Ag^+ from highly acidic wastewater," *Environmental Science: Nano*, vol. 6, pp. 3307–3315, 2019.

[37] Y. Wang and R. Liu, "H_2O_2 treatment enhanced the heavy metals removal by manure biochar in aqueous solutions," *Science of the Total Environment*, vol. 628–629, pp. 1139–1148, 2018.

[38] J. Jin, S. Li, X. Peng et al., "HNO_3 modified biochars for uranium (VI) removal from aqueous solution," *Bioresource Technology*, vol. 256, pp. 247–253, 2018.

[39] J. Li, B. Li, H. Huang et al., "Removal of phosphate from aqueous solution by dolomite-modified biochar derived from urban dewatered sewage sludge," *Science of the Total Environment*, vol. 687, pp. 460–469, 2019.

[40] M. Luo, H. Lin, B. Li, Y. Dong, Y. He, and L. Wang, "A novel modification of lignin on corncob-based biochar to enhance removal of cadmium from water," *Bioresource Technology*, vol. 259, pp. 312–318, 2018.

[41] X. Wang, Z. Guo, Z. Hu, H. H. Ngo, S. Liang, and J. Zhang, "Adsorption of phenanthrene from aqueous solutions by biochar derived from an ammoniation-hydrothermal method," *Science of the Total Environment*, vol. 733, article 139267, 2020.

[42] J. M. Salman, V. O. Njoku, and B. H. Hameed, "Batch and fixed-bed adsorption of 2,4-dichlorophenoxyacetic acid onto oil palm frond activated carbon," *Chemical Engineering Journal*, vol. 174, pp. 33–40, 2011.

[43] A. M. Soliman, H. M. Elwy, T. Thiemann, Y. Majedi, F. T. Labata, and N. A. F. Al-Rawashdeh, "Removal of Pb(II) ions from aqueous solutions by sulphuric acid-treated palm tree leaves," *Journal of the Taiwan Institute of Chemical Engineers*, vol. 58, pp. 264–273, 2016.

[44] S. M. Yakout and E. Elsherif, "Batch kinetics, isotherm and thermodynamic studies of adsorption of strontium from aqueous solutions onto low cost rice-straw based carbons," *Carbon-Science and Technology*, vol. 3, pp. 144–153, 2010.

[45] R. R. Bansode, J. N. Losso, W. E. Marshall, R. M. Rao, and R. J. Portier, "Pecan shell-based granular activated carbon for treatment of chemical oxygen demand (COD) in municipal wastewater," *Bioresource Technology*, vol. 94, no. 2, pp. 129–135, 2004.

[46] A. Gundogdu, C. Duran, H. B. Senturk et al., "Adsorption of phenol from aqueous solution on a low-cost activated carbon produced from tea industry waste: equilibrium, kinetic, and thermodynamic study," *Journal of Chemical and Engineering Data*, vol. 57, pp. 2733–2743, 2012.

[47] S. M. Yakout, A. A. M. Daifullah, and S. A. El-Reefy, "Adsorption of naphthalene, phenanthrene and pyrene from aqueous solution using low-cost activated carbon derived from agricultural wastes," *Adsorption Science and Technology*, vol. 31, pp. 293–302, 2013.

[48] L. Borah, M. Goswami, and P. Phukan, "Adsorption of methylene blue and eosin yellow using porous carbon prepared from tea waste: adsorption equilibrium, kinetics and thermodynamics study," *Journal of Environmental Chemical Engineering*, vol. 3, no. 2, pp. 1018–1028, 2015.

[49] B. Belhamdi, Z. Merzougui, M. Trari, and A. Addoun, "A kinetic, equilibrium and thermodynamic study of L-phenylalanine adsorption using activated carbon based on agricultural waste (date stones)," *Journal of Applied Research and Technology*, vol. 14, no. 5, pp. 354–366, 2016.

[50] M. Malhotra, S. Suresh, and A. Garg, "Tea waste derived activated carbon for the adsorption of sodium diclofenac from wastewater: adsorbent characteristics, adsorption isotherms, kinetics, and thermodynamics," *Environmental Science and Pollution Research*, vol. 25, pp. 32210–32220, 2018.

[51] O. A. Habeeb, O. A. Olalere, R. Kanthasamy, and B. V. Ayodele, "Hydrogen sulfide removal from downstream wastewater using calcium-coated wood sawdust-based activated carbon," *Arabian Journal for Science and Engineering*, vol. 45, pp. 501–518, 2020.

[52] T. A. Saleh, A. Sari, and M. Tuzen, "Optimization of parameters with experimental design for the adsorption of mercury using polyethylenimine modified-activated carbon," *Journal of Environmental Chemical Engineering*, vol. 5, pp. 1079–1088, 2017.

[53] Y. Xue, B. Gao, Y. Yao et al., "Hydrogen peroxide modification enhances the ability of biochar (hydrochar) produced from hydrothermal carbonization of peanut hull to remove aqueous heavy metals: batch and column tests," *Chemical Engineering Journal*, vol. 200–202, pp. 673–680, 2012.

[54] S. Banerjee, S. Mukherjee, A. LaminKa-ot, S. R. Joshi, T. Mandal, and G. Halder, "Biosorptive uptake of Fe^{2+}, Cu^{2+} and As^{5+} by activated biochar derived from *Colocasia esculenta*: isotherm, kinetics, thermodynamics, and cost estimation," *Journal of Advanced Research*, vol. 7, no. 5, pp. 597–610, 2016.

[55] X. J. Zuo, Z. Liu, and M. D. Chen, "Effect of H_2O_2 concentrations on copper removal using the modified hydrothermal biochar," *Bioresource Technology*, vol. 207, pp. 262–267, 2016.

[56] N. Zhao, C. Zhao, Y. Lv et al., "Adsorption and coadsorption mechanisms of Cr(VI) and organic contaminants on H3PO4 treated biochar," *Chemosphere*, vol. 186, pp. 422–429, 2017.

[57] S. Roy, S. Sengupta, S. Manna, and P. Das, "Chemically reduced tea waste biochar and its application in treatment of fluoride containing wastewater: batch and optimization using response surface methodology," *Process Safety and Environmental Protection*, vol. 116, pp. 553–563, 2018.

[58] Q. Wu, Y. Xian, Z. He et al., "Adsorption characteristics of Pb(II) using biochar derived from spent mushroom substrate," *Scientific Reports*, vol. 9, article 15999, pp. 1–11, 2019.

[59] L. Zhu, L. Tong, N. Zhao, J. Li, and Y. Lv, "Coupling interaction between porous biochar and nano zero valent iron/nano *A*-hydroxyl iron oxide improves the remediation efficiency of cadmium in aqueous solution," *Chemosphere*, vol. 219, pp. 493–503, 2019.

[60] S. Fan, J. Tang, Y. Wang et al., "Biochar prepared from co-pyrolysis of municipal sewage sludge and tea waste for the adsorption of methylene blue from aqueous solutions: kinetics, isotherm, thermodynamic and mechanism," *Journal of Molecular Liquids*, vol. 220, pp. 432–441, 2016.

[61] M. D. Huff and J. W. Lee, "Biochar-surface oxygenation with hydrogen peroxide," *Journal of Environmental Management*, vol. 165, pp. 17–21, 2016.

[62] K. Qiao, W. Tian, J. Bai et al., "Preparation of biochar from Enteromorpha prolifera and its use for the removal of polycyclic aromatic hydrocarbons (PAHs) from aqueous solution," *Ecotoxicology and Environmental Safety*, vol. 149, pp. 80–87, 2018.

[63] Q. Mao, Y. Zhou, Y. Yang et al., "Experimental and theoretical aspects of biochar-supported nanoscale zero-valent iron activating H_2O_2 for ciprofloxacin removal from aqueous solution," *Journal of Hazardous Materials*, vol. 380, article 120848, 2019.

[64] Y. Ma, H. Li, S. Zhang et al., "129Xe NMR: a powerful tool for studying the adsorption mechanism between mesoporous corn starch and palladium," *International Journal of Biological Macromolecules*, vol. 161, pp. 674–680, 2020.

[65] M. Ahmaruzzaman and S. L. Gayatri, "Activated tea waste as a potential low-cost adsorbent for the removal of *p*-nitrophenol from wastewater," *Journal of Chemical and Engineering Data*, vol. 55, pp. 4614–4623, 2010.

[66] S. Mandal, S. Pu, L. Shangguan et al., "Synergistic construction of green tea biochar supported nZVI for immobilization of lead in soil: a mechanistic investigation," *Environment International*, vol. 135, article 105374, 2020.

[67] D. Pal and S. K. Maiti, "Abatement of cadmium (Cd) contamination in sediment using tea waste biochar through meso-microcosm study," *Journal of Cleaner Production*, vol. 212, pp. 986–996, 2019.

[68] K. Amstaetter, E. Eek, and G. Cornelissen, "Sorption of PAHs and PCBs to activated carbon: coal versus biomass-based quality," *Chemosphere*, vol. 87, pp. 573–578, 2012.

[69] M. Ghaedi, M. Pakniat, Z. Mahmoudi, S. Hajati, R. Sahraei, and A. Daneshfar, "Synthesis of nickel sulfide nanoparticles loaded on activated carbon as a novel adsorbent for the competitive removal of methylene blue and safranin-O," *Spectrochimica Acta-Part A: Molecular and Biomolecular Spectroscopy*, vol. 123, pp. 402–409, 2014.

[70] M. Auta and B. H. Hameed, "Preparation of waste tea activated carbon using potassium acetate as an activating agent for adsorption of acid blue 25 dye," *Chemical Engineering Journal*, vol. 171, no. 2, pp. 502–509, 2011.

[71] A. Bazan-Wozniak and R. Pietrzak, "Adsorption of organic and inorganic pollutants on activated bio-carbons prepared by chemical activation of residues of supercritical extraction of raw plants," *Chemical Engineering Journal*, vol. 393, article 124785, 2020.

[72] A. Nasrullah, B. Saad, A. H. Bhat et al., "Mangosteen peel waste as a sustainable precursor for high surface area mesoporous activated carbon: characterization and application for methylene blue removal," *Journal of Cleaner Production*, vol. 211, pp. 1190–1200, 2019.

[73] A. Nasrullah, A. H. Bhat, A. Naeem, M. H. Isa, and M. Danish, "High surface area mesoporous activated carbon-alginate beads for efficient removal of methylene blue," *International Journal of Biological Macromolecules*, vol. 107, pp. 1792–1799, 2018.

[74] B. Maazinejad, O. Mohammadnia, G. A. M. Ali et al., "Taguchi L9 (34) orthogonal array study based on methylene blue removal by single-walled carbon nanotubes-amine: adsorption optimization using the experimental design method,

kinetics, equilibrium and thermodynamics," *Journal of Molecular Liquids*, vol. 298, article 112001, 2020.

[75] H. Kk, A. Rm, H. Ms, Z. De, and K. Mh, "Preparation of activated carbon from waste cooked tea for using as chemical dyes-filter," in *IC onTES 2018 : International Conference on Technology, Engineering and Science*, pp. 15–20, 2018.

[76] B. Okoro and N. Nwaiwu, "COD and nutrient removal kinetics of piggery wastewater in Nigeria," *Journal of Scientific Research and Reports*, vol. 16, pp. 1–9, 2017.

[77] G. Cazaudehore, B. Schraauwers, C. Peyrelasse, C. Lagnet, and F. Monlau, "Determination of chemical oxygen demand of agricultural wastes by combining acid hydrolysis and commercial COD kit analysis," *Journal of Environmental Management*, vol. 250, article 109464, 2019.

[78] J. Lu, X. Wang, B. Shan, X. Li, and W. Wang, "Analysis of chemical compositions contributable to chemical oxygen demand (COD) of oilfield produced water," *Chemosphere*, vol. 62, pp. 322–331, 2006.

[79] E. Mohammad-pajooh, A. E. Turcios, G. Cuff et al., "Removal of inert COD and trace metals from stabilized landfill leachate by granular activated carbon (GAC) adsorption," *Journal of Environmental Management*, vol. 228, pp. 189–196, 2018.

[80] A. A. Halim, H. A. Aziz, M. A. M. Johari, K. S. Ariffin, and M. N. Adlan, "Ammoniacal nitrogen and COD removal from semi-aerobic landfill leachate using a composite adsorbent: fixed bed column adsorption performance," *Journal of Hazardous Materials*, vol. 175, pp. 960–964, 2010.

[81] A. A. Halim, H. A. Aziz, M. A. M. Johari, and K. S. Ariffin, "Comparison study of ammonia and COD adsorption on zeolite, activated carbon and composite materials in landfill leachate treatment," *Desalination*, vol. 262, no. 1–3, pp. 31–35, 2010.

[82] R. Devi, V. Singh, and A. Kumar, "COD and BOD reduction from coffee processing wastewater using Avacado peel carbon," *Bioresource Technology*, vol. 99, no. 6, pp. 1853–1860, 2008.

[83] D. Mohan, K. P. Singh, and V. K. Singh, "Wastewater treatment using low cost activated carbons derived from agricultural byproducts — a case study," *Journal of Hazardous materials*, vol. 152, pp. 1045–1053, 2008.

[84] Y. M. Tang, M. Junaid, A. Niu, S. Deng, and D. S. Pei, "Diverse toxicological risks of PAHs in surface water with an impounding level of 175 m in the three gorges reservoir area, China," *Science of the Total Environment*, vol. 580, pp. 1085–1096, 2017.

[85] P. Oleszczuk, S. E. Hale, J. Lehmann, and G. Cornelissen, "Activated carbon and biochar amendments decrease porewater concentrations of polycyclic aromatic hydrocarbons (PAHs) in sewage sludge," *Bioresource Technology*, vol. 111, pp. 84–91, 2012.

[86] M. Hosseinpour, M. Akizuki, Y. Oshima, and M. Soltani, "Influence of formic acid and iron oxide nanoparticles on active hydrogenation of PAHs by hot compressed water. Isotope tracing study," *Fuel*, vol. 254, article 115675, 2019.

[87] A. Malakahmad, M. X. Law, K. W. Ng, and T. S. A. Manan, "The fate and toxicity assessment of polycyclic aromatic hydrocarbons (PAHs) in water streams of Malaysia," *Procedia Engineering*, vol. 148, pp. 806–811, 2016.

[88] M. A. Nkansah, A. A. Christy, T. Barth, and G. W. Francis, "The use of lightweight expanded clay aggregate (LECA) as sorbent for PAHs removal from water," *Journal of Hazardous Materials*, vol. 217–218, pp. 360–365, 2012.

[89] C. Zhang, J. Lu, and J. Wu, "Adsorptive removal of polycyclic aromatic hydrocarbons by detritus of green tide algae deposited in coastal sediment," *Science of the Total Environment*, vol. 670, pp. 320–327, 2019.

[90] J. A. Kumar, D. J. Amarnath, S. Sathish et al., "Enhanced PAHs removal using pyrolysis-assisted potassium hydroxide induced palm shell activated carbon: batch and column investigation," *Journal of Molecular Liquids*, vol. 279, pp. 77–87, 2019.

[91] C. Valderrama, X. Gamisans, X. Heras, A. Farran, and J. L. Cortina, "Sorption kinetics of polycyclic aromatic hydrocarbons removal using granular activated carbon: intraparticle diffusion coefficients," *Journal of Hazardous Materials*, vol. 157, pp. 386–396, 2008.

[92] Y. Huang, A. N. Fulton, and A. A. Keller, "Simultaneous removal of PAHs and metal contaminants from water using magnetic nanoparticle adsorbents," *Science of the Total Environment*, vol. 571, pp. 1029–1036, 2016.

[93] Z. Hao, C. Wang, Z. Yan, H. Jiang, and H. Xu, "Magnetic particles modification of coconut shell-derived activated carbon and biochar for effective removal of phenol from water," *Chemosphere*, vol. 211, pp. 962–969, 2018.

[94] Z. Yang, C. Gan, X. Feng, G. Cai, J. Zhang, and H. Ji, "Imidazolium-functionalized stable gel materials for efficient adsorption of phenols from aqueous solutions," *Environmental Technology and Innovation*, vol. 17, article 100511, 2020.

[95] J. W. Lim, H. F. Mohd Zaid, M. H. Isa et al., "Shielding immobilized biomass cryogel beads with powdered activated carbon for the simultaneous adsorption and biodegradation of 4-chlorophenol," *Journal of Cleaner Production*, vol. 205, pp. 828–835, 2018.

[96] J. H. Park, J. J. Wang, Y. Meng, Z. Wei, R. D. DeLaune, and D. C. Seo, "Adsorption/desorption behavior of cationic and anionic dyes by biochars prepared at normal and high pyrolysis temperatures," *Colloids and Surfaces A: Physicochemical and Engineering Aspects*, vol. 572, pp. 274–282, 2019.

[97] T. M. Huggins, A. Haeger, J. C. Biffinger, and Z. J. Ren, "Granular biochar compared with activated carbon for wastewater treatment and resource recovery," *Water Research*, vol. 94, pp. 225–232, 2016.

[98] M. M. Manyuchi, C. Mbohwa, and E. Muzenda, "Feasibility of using sewage sludge bio char in treating municipal sewage," in *Proceedings of the International Conference on Industrial Engineering and Operations Management*, vol. 2018, pp. 44–50, Washington DC, USA, 2018.

[99] A. S. Khalil, A. S. Smolyanichenko, E. V. Vilson, E. E. Shchutskaya, E. G. Tsurikova, and A. S. Khalil, "Modeling of ammonium and COD adsorption in aqueous solutions using an artificial neural," *Network*, vol. 1, pp. 212–218, 2019.

[100] P. Oleszczuk, A. Zielińska, and G. Cornelissen, "Stabilization of sewage sludge by different biochars towards reducing freely dissolved polycyclic aromatic hydrocarbons (PAHs) content," *Bioresource Technology*, vol. 156, pp. 139–145, 2014.

[101] K. Yang, Y. Jiang, J. Yang, and D. Lin, "Correlations and adsorption mechanisms of aromatic compounds on biochars produced from various biomass at 700°C," *Environmental Pollution*, vol. 233, pp. 64–70, 2018.

[102] X. Chen, L. Yang, S. C. B. Myneni, and Y. Deng, "Leaching of polycyclic aromatic hydrocarbons (PAHs) from sewage sludge-derived biochar," *Chemical Engineering Journal*, vol. 373, pp. 840–845, 2019.

[103] P. Godlewska, A. Siatecka, M. Kończak, and P. Oleszczuk, "Adsorption capacity of phenanthrene and pyrene to engineered carbon-based adsorbents produced from sewage sludge or sewage sludge-biomass mixture in various gaseous conditions," *Bioresource Technology*, vol. 280, pp. 421–429, 2019.

[104] G. L. Sullivan, R. M. Prigmore, P. Knight, and A. R. Godfrey, "Activated carbon biochar from municipal waste as a sorptive agent for the removal of polyaromatic hydrocarbons (PAHs), phenols and petroleum based compounds in contaminated liquids," *Journal of Environmental Management*, vol. 251, article 109551, 2019.

[105] H. Cheng, R. Ji, Y. Bian, X. Jiang, and Y. Song, "From macroalgae to porous graphitized nitrogen-doped biochars – using aquatic biota to treat polycyclic aromatic hydrocarbons-contaminated water," *Bioresource Technology*, vol. 303, article 122947, 2020.

[106] H. Jia, J. Li, Y. Li, H. Lu, J. Liu, and C. Yan, "The remediation of PAH contaminated sediment with mangrove plant and its derived biochars," *Journal of Environmental Management*, vol. 268, article 110410, pp. 1–8, 2020.

[107] M. Naghdi, M. Taheran, R. Pulicharla et al., "Pine-wood derived nanobiochar for removal of carbamazepine from aqueous media: adsorption behavior and influential parameters," *Arabian Journal of Chemistry*, vol. 12, pp. 5292–5301, 2019.

[108] H. Qiao, L. Mei, G. Chen et al., "Adsorption of nitrate and phosphate from aqueous solution using amine cross-linked tea wastes," *Applied Surface Science*, vol. 483, pp. 114–122, 2019.

[109] S. Wan, Z. Hua, L. Sun, X. Bai, and L. Liang, "Biosorption of nitroimidazole antibiotics onto chemically modified porous biochar prepared by experimental design: kinetics, thermodynamics, and equilibrium analysis," *Process Safety and Environmental Protection*, vol. 104, pp. 422–435, 2016.

[110] T. Chen, L. Luo, S. Deng et al., "Sorption of tetracycline on H_3PO_4 modified biochar derived from rice straw and swine manure," *Bioresource Technology*, vol. 267, pp. 431–437, 2018.

[111] P. Liu, W. J. Liu, H. Jiang, J. J. Chen, W. W. Li, and H. Q. Yu, "Modification of bio-char derived from fast pyrolysis of biomass and its application in removal of tetracycline from aqueous solution," *Bioresource Technology*, vol. 121, pp. 235–240, 2012.

[112] A. C. Martins, O. Pezoti, A. L. Cazetta et al., "Removal of tetracycline by NaOH-activated carbon produced from macadamia nut shells: kinetic and equilibrium studies," *Chemical Engineering Journal*, vol. 260, pp. 291–299, 2015.

[113] H. M. Jang, S. Yoo, Y. K. Choi, S. Park, and E. Kan, "Adsorption isotherm, kinetic modeling and mechanism of tetracycline on *Pinus taeda*-derived activated biochar," *Bioresource Technology*, vol. 259, pp. 24–31, 2018.

[114] X. Zhu, C. Li, J. Li, B. Xie, J. Lü, and Y. Li, "Thermal treatment of biochar in the air/nitrogen atmosphere for developed mesoporosity and enhanced adsorption to tetracycline," *Bioresource Technology*, vol. 263, pp. 475–482, 2018.

[115] V. T. Nguyen, T. B. Nguyen, C. W. Chen, C. M. Hung, C. P. Huang, and C. DongDi, "Cobalt-impregnated biochar (Co-SCG) for heterogeneous activation of peroxymonosulfate for removal of tetracycline in water," *Bioresource Technology*, vol. 292, article 121954, 2019.

[116] J. Luo, X. Li, C. Ge et al., "Sorption of norfloxacin, sulfamerazine and oxytetracycline by KOH-modified biochar under single and ternary systems," *Bioresource Technology*, vol. 263, pp. 385–392, 2018.

[117] J. Heo, Y. Yoon, G. Lee, Y. Kim, J. Han, and C. M. Park, "Enhanced adsorption of bisphenol A and sulfamethoxazole by a novel magnetic $CuZnFe_2O_4$–biochar composite," *Bioresource Technology*, vol. 281, pp. 179–187, 2019.

[118] T. Madrakian, A. Afkhami, and M. Ahmadi, "Adsorption and kinetic studies of seven different organic dyes onto magnetite nanoparticles loaded tea waste and removal of them from wastewater samples," *Spectrochimica Acta-Part A: Molecular and Biomolecular Spectroscopy*, vol. 99, pp. 102–109, 2012.

[119] H. Dong, C. Zhang, K. Hou et al., "Removal of trichloroethylene by biochar supported nanoscale zero-valent iron in aqueous solution," *Separation and Purification Technology*, vol. 188, no. 9, pp. 188–196, 2017.

[120] H. Khoshsang and A. Ghaffarinejad, "Rapid removal of lead (II) ions from aqueous solutions by saffron flower waste as a green biosorbent," *Journal of Environmental Chemical Engineering*, vol. 6, no. 5, pp. 6021–6027, 2018.

[121] M. Hasnain Isa, L. Siew Lang, F. A. H. Asaari, H. A. Aziz, N. Azam Ramli, and J. P. A. Dhas, "Low cost removal of disperse dyes from aqueous solution using palm ash," *Dyes and Pigments*, vol. 74, no. 2, pp. 446–453, 2007.

[122] R. Asadpour, N. B. Sapari, M. H. Isa, and K. U. Orji, "Enhancing the hydrophobicity of mangrove bark by esterification for oil adsorption," *Water Science and Technology*, vol. 70, pp. 1220–1228, 2014.

[123] A. R. Rahmani, E. Hossieni, and A. Poormohammadi, "Removal of chromium (VI) from aqueous solution using oil palm ash," *Environmental Processes*, vol. 2, pp. 419–428, 2015.

[124] H. Khurshid, M. R. U. Mustafa, U. Rashid, M. H. Isa, H. Y. Chia, and M. M. Shah, "Adsorptive removal of COD from produced water using tea waste biochar," *Environmental Technology & Innovation*, vol. 23, article 101563, 2021.

[125] L. Liu, W. Cui, C. Lu et al., "Analyzing the adsorptive behavior of amoxicillin on four Zr-MOFs nanoparticles: functional groups dependence of adsorption performance and mechanisms," *Journal of Environmental Management*, vol. 268, article 110630, 2020.

[126] A. Gallo-Cordova, M. D. M. Silva-Gordillo, G. A. Muñoz, X. Arboleda-Faini, and D. Almeida Streitwieser, "Comparison of the adsorption capacity of organic compounds present in produced water with commercially obtained walnut shell and residual biomass," *Journal of Environmental Chemical Engineering*, vol. 5, no. 4, pp. 4041–4050, 2017.

[127] L. Kong and H. Adidharma, "A new adsorption model based on generalized van der Waals partition function for the description of all types of adsorption isotherms," *Chemical Engineering Journal*, vol. 375, article 122112, 2019.

[128] M. Khalfaoui, S. Knani, M. A. Hachicha, and A. B. Lamine, "New theoretical expressions for the five adsorption type isotherms classified by BET based on statistical physics treatment," *Journal of Colloid and Interface Science*, vol. 263, pp. 350–356, 2003.

[129] M. Sultan, T. Miyazaki, and S. Koyama, "Optimization of adsorption isotherm types for desiccant air-conditioning applications," *Renewable Energy*, vol. 121, pp. 441–450, 2018.

[130] M. A. Mosquera, "Simple isotherm equations to fit type I adsorption data," *Fluid Phase Equilibria*, vol. 337, pp. 174–182, 2013.

[131] J. Samuelsson, T. Undin, and T. Fornstedt, "Expanding the elution by characteristic point method for determination of various types of adsorption isotherms," *Journal of Chromatography A*, vol. 1218, pp. 3737–3742, 2011.

[132] T. Kohler, M. Hinze, K. Müller, and W. Schwieger, "Temperature independent description of water adsorption on zeotypes showing a type V adsorption isotherm," *Energy*, vol. 135, pp. 227–236, 2017.

[133] S. Yurdakal, C. Garlisi, L. Özcan, M. Bellardita, and G. Palmisano, "(Photo)catalyst characterization techniques: adsorption isotherms and BET, SEM, FTIR, UV-Vis, photoluminescence, and electrochemical characterizations," in *Heterogeneous Photocatalysis: Relationships with Heterogeneous Catalysis and Perspectives*, Elsevier, 2019.

[134] H. Pang, Z. Diao, X. Wang et al., "Adsorptive and reductive removal of U(VI) by *Dictyophora indusiate*-derived biochar supported sulfide NZVI from wastewater," *Chemical Engineering Journal*, vol. 366, pp. 368–377, 2019.

[135] X. Lu, F. Wang, X. Y. Li, K. Shih, and E. Y. Zeng, "Adsorption and thermal stabilization of Pb^{2+} and Cu^{2+} by zeolite," *Industrial and Engineering Chemistry Research*, vol. 55, pp. 8767–8773, 2016.

[136] Y. Priastomo, H. R. Setiawan, Y. S. Kurniawan, and K. Ohto, "Simultaneous removal of lead(II), chromium(III), and copper(II) heavy metal ions through an adsorption process using C-phenylcalix[4]pyrogallolarene material," *Journal of Environmental Chemical Engineering*, vol. 8, article 103971, 2020.

[137] T. Khan, T. Sabariah, B. Abd et al., "Modeling of Cu(II) adsorption from an aqueous solution using an artificial neural network (ANN)," *Molecules*, vol. 25, no. 14, p. 3263, 2020.

[138] A. Shahzad, K. Rasool, W. Miran et al., "Two-dimensional $Ti_3C_2T_x$ MXene nanosheets for efficient copper removal from water," *ACS Sustainable Chemistry and Engineering*, vol. 5, pp. 11481–11488, 2017.

[139] H. Sun and Z. Zhou, "Impacts of charcoal characteristics on sorption of polycyclic aromatic hydrocarbons," *Chemosphere*, vol. 71, pp. 2113–2120, 2008.

[140] O. Mashtalir, K. M. Cook, V. N. Mochalin, M. Crowe, M. W. Barsoum, and Y. Gogotsi, "Dye adsorption and decomposition on two-dimensional titanium carbide in aqueous media," *Journal of Materials Chemistry A*, vol. 2, pp. 14334–14338, 2014.

[141] P. Shao, L. Ding, J. Luo et al., "Lattice-defect-enhanced adsorption of arsenic on zirconia nanospheres: a combined experimental and theoretical study," *ACS Applied Materials and Interfaces*, vol. 11, pp. 29736–29745, 2019.

[142] Z. Wan, D. W. Cho, D. C. W. Tsang, M. Li, T. Sun, and F. Verpoort, "Concurrent adsorption and micro-electrolysis of Cr(VI) by nanoscale zerovalent iron/biochar/Ca-alginate composite," *Environmental Pollution*, vol. 247, pp. 410–420, 2019.

[143] S. Mandal, A. Kunhikrishnan, N. S. Bolan, H. Wijesekara, and R. Naidu, "Application of biochar produced from biowaste materials for environmental protection and sustainable agriculture production," in *Environmental Materials and Waste: Resource Recovery and Pollution Prevention*, Elsevier Inc., 2016.

[144] L. Liu, Y. Huang, Y. Meng et al., "Investigating the adsorption behavior and quantitative contribution of Pb^{2+} adsorption mechanisms on biochars by different feedstocks from a fluidized bed pyrolysis system," *Environmental Research*, vol. 187, article 109609, 2020.

[145] K. L. B. Solis, Y. H. Kwon, M. H. Kim, H. R. An, C. Jeon, and Y. Hong, "Metal organic framework UiO-66 and activated carbon composite sorbent for the concurrent adsorption of cationic and anionic metals," *Chemosphere*, vol. 238, article 124656, 2020.

[146] C. S. Patil, D. B. Gunjal, V. M. Naik et al., "Waste tea residue as a low cost adsorbent for removal of hydralazine hydrochloride pharmaceutical pollutant from aqueous media: an environmental remediation," *Journal of Cleaner Production*, vol. 206, pp. 407–418, 2019.

[147] Y. Shi, H. Hu, and H. Ren, "Dissolved organic matter (DOM) removal from biotreated coking wastewater by chitosan-modified biochar: adsorption fractions and mechanisms," *Bioresource Technology*, vol. 297, article 122281, 2020.

[148] U. Rashid, J. Ahmad, M. L. Ibrahim, J. Nisar, M. A. Hanif, and T. Y. C. Shean, "Single-pot synthesis of biodiesel using efficient sulfonated-derived tea waste-heterogeneous catalyst," *Materials*, vol. 12, pp. 1–16, 2019.

[149] Q. Zhang, D. Zhang, H. Xu et al., "Biochar filled high-density polyethylene composites with excellent properties: towards maximizing the utilization of agricultural wastes," *Industrial Crops and Products*, vol. 146, article 112185, 2020.

[150] C. G. Lee, S. Lee, J. A. Park et al., "Removal of copper, nickel and chromium mixtures from metal plating wastewater by adsorption with modified carbon foam," *Chemosphere*, vol. 166, pp. 203–211, 2017.

[151] L. Qian, S. Liu, W. Zhang et al., "Enhanced reduction and adsorption of hexavalent chromium by palladium and silicon rich biochar supported nanoscale zero-valent iron," *Journal of Colloid and Interface Science*, vol. 533, pp. 428–436, 2019.